Improving Techniques for Cell Implantation and their Impact on Managing Diseases of the Pancreas

by

Nasser Abualhassan

A thesis submitted in partial fulfillment of the requirements for the degree of

Master of Science

in

Experimental Surgery

Department of Surgery

University of Alberta

Abstract

The use of experimental animals early in the twentieth century has revolutionized medicine and significantly improved our understanding of disease processes. The ability to reproduce a medical condition in a mouse model has provided great insights into the cellular and molecular biology of the disease process and a valuable medium to develop and test therapy that would eventually be translated into the clinic. Cell implantation has been utilized extensively in cancer research and has resulted in remarkable progress in cancer therapy especially in leukemia. Cellular transplantation has also proven valuable as a replacement therapy such as in type 1 diabetes. A major barrier to successfully translate the observation in a mouse model to the clinic is the ability to generate a relevant mouse model that accurately represents the clinical condition of interest.

The objective of this graduate work is to study the existing cellular implantation animal models in an attempt to modify and improve the techniques used for cellular implantation. In the first part of this thesis, we utilized a novel prevascularized subcutaneous site, developed in our laboratory, for pancreatic cancer xenograft. This approach accelerated tumor growth in our immunodeficient mouse model, which would have a great clinical value when implemented in personalized medicine. Taking advantage of the accelerated tumor growth, characterization and drug testing of the tumor can be done in time to direct therapy in the clinic for individual patients.

In the second part of this thesis, we have utilized a novel transplantation method for pancreatic islet transplantation to treat diabetes. In this method, islets are seeded on micro organ-derived scaffolds and subsequently implanted into the peritoneal cavity of immunodeficient mice. This approach restores the islet microenvironment by providing a wide variety of extracellular matrix proteins that resulted in a significant reduction of the required islet mass in an extravascular site. This could be of a great clinical value given the potential of transplanting more than one recipient with one donor organ.

Preface

Chapter 1 of this thesis was submitted to *Current Oncology* 2016 for publication. I have conducted a review of pancreatic cancer and experimental animal research. A. Bruni contributed to the literature review. A.M.J Shapiro contributed to critical review of the manuscript.

Chapter 2 of this thesis was submitted to *Pancreas* 2016 for publication. I was involved in designing, conducting, collection and interpretation of all experiments as well as writing the manuscript. A. Bruni and M. Bral contributed to cell implantation. R. Pawlick and B. Gala-Lopez contributed to the study design and data interpretation. A. Pepper contributed to data analysis and critical review of the study. A.M.J Shapiro contributed to study design, data interpretation and critical review of the manuscript.

Chapter 4 of this thesis has been published in *PLOS ONE* 2016. This chapter was a part of collaboration with Dr. Eduardo Mitrani from the Hebrew University of Jerusalem, Israel. I was involved in designing, conducting, collection and interpretation of all experiments as well as writing the manuscript. R. Pawlick, A. Bruni and A. Pepper contributed to islet isolation and transplantation. L. Sapozhnikove and M. Kahana contributed to preparation of the scaffolds. B. Gala-Lopez and A. Pepper contributed to data analysis and interpretation. T. Kin contributed to human islet isolation. E. Mitrani and A.M.J Shapiro contributed to study design, data interpretation and critical review of the manuscript.

This thesis is an original work by Nasser Abualhassan. The research project, of which

this thesis is a part, received research ethics approval from Health Research Ethic Board – Biomedical Panel of the University of Alberta (Study ID: Pro00041552) and the University of Alberta Research Ethic and Animal Use Committee (Study ID: AUP00000419 & AUP00000991).

Dedication

I dedicate this thesis to my family. Without their love and support this work would not have been possible.

Acknowledgements

I am truly thankful to have had the opportunity to do my graduate studies under the supervision and guidance of Dr. Shapiro. It has been a privilege to have been exposed to his mentorship and inspiration that have been paramount to overcoming any obstacles I may have encountered and in formulating any success I had. I will always be profoundly indebted to him.

I have been extremely fortunate to be surrounded by the wonderful members of Shapiro's lab. They all have been great friends and mentors. It would not have been possible to have completed this journey without their help and support. I would like to thank my friends: Rena Pawlick, Andrew Pepper, Antonio Bruni, Boris Gala-Lopez and Mariusz Bral who have contributed to my success and for which I will be forever grateful.

I would like to thank Dr. Adetola Adesida, who had accepted to chair my defense with a very short notice. I must also thank Dr. Thomas Churchill and all the members of the Department of Surgery. A special thanks to my Advisory Committee: Dr. Colin Anderson and Dr. Michael Sawyer. Their support and guidance have contributed significantly to my progression and success. I would like to also thank all of our collaborators especially Dr. Vijaya Damaraju and Dr. Melinda Wuest for their help and support.

Finally, without the inspiration and support of my family it would have been impossible to achieve any success. Thank you all for being always there for me.

Table of Contents

List of Tables

List of Figures

List of Abbreviations

Abbreviation	Meaning
ATCC	American Type Culture Collection
AUC	Area under the curve
BM	Basement membrane
BMI	Body mass index
BOP	N-nitrosobis(2-oxopropyl)-amine
BRAC2	Breast cancer 2
Col	Collagen
CRP	C-reactive protein
3D	Three-dimensional
DAPI	45-diamidino-2-phenylindole
DIPN	Diisopropanolnitrosamine
DL	Device-Less
DMBA	7,12-dimethylbenz[a]anthracene
DMEM	Dulbecco's Minimal Essential Medium
DNA	Deoxyribonucleic acid
DPP-4	Dipeptidyl peptidase-4
ECM	Extra-cellular matrix
EDTA	Ethylene-diamine-tetraacetic acid
EGFR	Epidermal growth factor receptor
ELISA	Enzyme-linked immunosorbent assay
EMP	Engineered micro-pancreas

FAMMM	Familial atypical multiple mole melanoma syndrome
FDA	Food and Drug Administration
FLT	3`-deoxy-3`-fluorothymidine
GFP	Green fluorescent protein
GLP-1	Glucagon-like peptide 1
hENT-1	Human Equilibrative Nucleoside Transporter
HBSS	Hank's Balanced Salt Solution
HGF	Hepatocyte growth factor
HNPCC	Hereditary non-polyposis colorectal cancer
IBMIR	Instant blood mediated inflammatory reaction
IEQ	Islet equivalents
IL	Interleukin
IAPP	Islet associated polypeptides
IP	Intraperitoneal
IPGTTs	Intraperitoneal glucose tolerance tests
IPMN	Intraductal papillary mucinous neoplasms
KC/GRO	Keratinocyte growth factor
Milli-Q	Double distilled deionized water
MS	Mass spectrometry
NBMPR	Nitrobenzylmercaptopurine ribonucleoside
NF-κB	Nuclear factor-κB
NOD	Non-obese diabetic
NSG	Non-obese diabetic/severe combined immunodeficiency

OR	Odds ratio
PAHs	Polycyclic aromatic hydrocarbons
PET	Positron emission tomography
PDX	Patient-derived xenograft
PLGA	Poly(lactide-co-glycolide)
SCID	Severe combined immunodeficiency
SEM	Standard error of the mean
SQ	Subcutaneous
T1DM	Type 1 diabetes mellitus
TNF-α	Tumor necrosis factor - α
TUNEL	Dexoynucleotidyl transferase dUTP nick end labeling
VEGF-A	Vascular endothelial growth factor - A
VEGF-C	Vascular endothelial growth factor – C

Chapter 1

Pancreatic Cancer and Advances in Experimental Animal Research

1.1 Introduction

Pancreatic cancer is considered among the most lethal of malignancies with an extremely poor prognosis even when discovered at an early stage. It is the fourth leading cause of death from cancer, with over 46,000 new cases and 39,000 deaths occurring every year.(1) In Canada, it is estimated that 4,800 new patients will be diagnosed with pancreatic cancer in 2015, 4,600 of them will die within one year of diagnosis.(2) The etiology of pancreatic cancer is poorly understood. Approximately 95% of pancreatic cancers are exocrine in origin, of which, ductal adenocarcinoma is the most common entity, accounting for 75 to 90% of cases.(2) Many risk factors have been linked to pancreatic cancer, including but not limited to smoking, obesity, long standing diabetes mellitus, chronic pancreatitis and genetic syndromes.(3). Heavy alcohol consumption high caloric intake, infrequent vegetable consumption and occupational exposure to chlorinated hydrocarbon compounds and polycyclic aromatic hydrocarbons (PAHs) have also been linked to development of pancreatic cancer.(4) Currently, surgical resection offers the only potential cure, with a 5-year survival approaching 14% at best.(2) However, less than 10% of tumors are resectable at the time of diagnosis(5), largely attributed to the retroperitoneal location of the pancreas, as well as the lack of early symptoms and biological markers. In more than 80% of cases, the cancer has advanced beyond resection at the time of diagnosis. The average overall survival duration ranges

from 4 to 6 months, with 5-year survival at less than 5%.(6) Promising results of therapeutic regimens in laboratory and mouse models often fail or have little effects when translated to clinical trials.(7, 8) Most of the animal xenograft models that have been used for drug testing and development had utilized well-established cell lines that are implanted into immunodeficient mice.(7, 8) The lack of clinically relevant animal models that can reliably predict outcomes in human has lead to development of a direct xenograft mouse model.(9) In this model, freshly resected tumor tissue is implanted within hours into immunodeficient mice. Utilizing this approach has been proven to preserve the histology and gene expression of the original cancer.(10, 11) In this review, we focus on the advances in animal model development and the utility of such models in treatment of pancreatic cancer.

1.2 Historical Perspective

Pancreatic cancer was first recognized in 1679 when 5 cases were published in the Sepulchretum of Bonet by Morgagni.(12, 13) The clinical presentation had become well-known by the end of the 19th century with many histologically proven cases.(12) The first solid tumor resection from the body of the pancreas was probably performed by Trendelenburg in 1882 for a spindle cell sarcoma.(14) Codivilla had performed a surgical resection of most of the duodenum and head of the pancreas for pancreatic cancer in 1898. However, the patient died about 3 weeks after surgery. The first successful resection of a tumor involving the ampulla of Vater was performed by William S. Halsted in 1898.(12) Kausch was the first to perform a successful two stage

pancreaticoduodenctomy and the patient survived for about 9 months after surgery.(12) In 1937, Alexander, Brunschwig performed a wide resection of the duodenum and head of the pancreas in two stages for pancreatic head cancer.(14)

On March 1940, Allen Oldfather Whipple and Nelson were the first to perform a successful one-stage resection of the head of the pancreas and duodenum in New York for pancreatic islet tumor of the head of the pancreas. The procedure involved partial gastrectomy in addition to the pancreaticoduodenectomy.(12, 15) Whipple's one-stage surgery has become the standard procedure for cancers involving the head of the pancreas or the duodenum.(15) Over the years, the mortality rate of the Whipple's procedure has declined from over 50% to less than 5%. This improvement was initially due to the transition to non-absorbable silk sutures for the pancreatic reconstruction, which were more resistant than catgut to enzymatic degradation and anastomotic breakdown. Subsequent survival improvements reflect modern advances in surgical technique, anesthesia and post-operative care. However, the 5-year survival rate still remains under 20 %.(2, 16)

1.3 Risk Factors of Pancreatic Cancer

It has been documented that the most common risk factor for development of pancreatic cancer is smoking, which has been associated with up to 25% of all cases.(17) It increases the risk by at least 2-fold compared to non-smokers.(3) This risk decreases significantly after smoking cessation.(18) Long standing diabetes mellitus has become recently linked to development of pancreatic cancer with up to a 2-fold risk increase.(3,

19, 20) It is not clear whether diabetes is a cause or a consequence of pancreatic cancer. One study has shown that 1% of patients with new onset diabetes, over the age of 50, will develop pancreatic cancer.(21) On the other hand, it is possible that long term exposure to insulin may contribute to the development of the disease through growth factor activation.(22) Patients who received exogenous insulin therapy for diabetes treatment have a significantly higher risk of pancreatic cancer, as compared to patients who did not receive insulin.(23) A recent meta-analysis of the use of the type 2 diabetes drug metformin, exhibited a significant reduction in the risk of developing pancreatic cancer compared to other anti-diabetic drugs.(24) Obesity has also been linked to pancreatic cancer, which may exert its effect through insulin resistance.(3, 4)

In a congenitally obese mouse model of pancreatic cancer, mice were implanted with the PAN02 cell line. Obesity was subsequently induced by diet and resulted in accelerated cancer growth with significantly elevated circulating insulin.(25) Clinically, it is estimated that the risk of cancer increases for every 5 kg/m^2 increment in BMI as an independent risk factor.(26) Early adulthood obesity is associated with even higher risk probably by exposing the pancreas to higher levels of insulin for a prolong period.(27) High caloric intake has also been linked to pancreatic cancer.(4, 28) High fat content seems to act as a promoter for carcinogenesis.(29) Conversely, high fruit intake seems to have a protective effect.(30) In a hamster model, high fat-fed animals had a 3-fold increase in the incidence of cancer after they were injected with N-nitrosobis-(2-oxopropyl)amine compared to control.(31)

Family history of pancreatic cancer is a significant risk factor in the development of pancreatic cancer.(3) Familial pancreatic cancer refers to families with a minimum of 2

first-degree relatives with confirmed pancreatic cancer with no known history of other inherited tumor syndromes.(32) It is estimated that 5-10% of pancreatic cancers are hereditary.(33) In addition, several known tumor syndromes have been associated with pancreatic cancers including hereditary pancreatitis, familial breast cancer syndrome (BRCA2), Peutz-Jeghers syndrome, hereditary non-polyposis colorectal cancer (HNPCC) and familial atypical multiple mole melanoma syndrome (FAMMM) and hereditary pancreatitis.(3, 32, 33)

History of pancreatitis significantly increases the risk for development of pancreatic cancer. The risk of pancreatic cancer in chronic pancreatitis is increased up to 20-fold.(34) A recent pooled analysis of 5048 cases of ductal pancreatic adenocarcinoma have shown a three-fold increased risk at intervals of less than two years and about 13-fold increased risk at intervals of more than two years (OR: 2.71 and 13.56 respectively).(35) Over a 20 year period, about 5% of patients with chronic pancreatitis will develop pancreatic cancer.(36) Heavy alcohol abuse (≥ 3 dinks/day) has also been associated with pancreatic cancer (relative risk 1.36 to 1.62).(37, 38) However, smoking and other confounding factors cannot be completely excluded.(37, 38)

Glucagon-like peptide 1 (GLP-1), is a very short acting peptide hormone secreted by intestinal epithelial endocrine L-cells, and it has a stimulatory effect on islet β-cells and an inhibitory effect on α-cells.(39) Animal studies have demonstrated a link between pancreatitis and the use of GLP-1 mimetic medications, which could eventually increase the risk of cancer.(40-43) In a study by Elashoff et al., the risk of pancreatitis was increased by 6-fold in patients treated with GLP-1 mimetic drugs, exenatide and sitagliptin, from the analysis of data obtained from FDA adverse events reporting. It

could potentially increase the risk of pancreatic cancer through insulin release and pancreatitis.

Chlorinated hydrocarbon compounds and polycyclic aromatic hydrocarbons (PAHs) are among the strongest contributors to the development of pancreatic cancer. For PAHs exposure, aluminum production and metalworking industries have shown consistent elevated risks.(44, 45)

1.4 Animal Models for Pancreatic Cancer

The pathogenesis of pancreatic cancer is poorly understood. The knowledge obtained from cell culture studies have contributed significantly to our understanding of the disease. It is of special importance in complex tissues where cells can be dissociated and studied individually. Improvements in culturing techniques and cryopreservation have provided the means of establishing cell lines.(46) Many studies have been performed using animal models with different strategies of disease to simulate pancreatic cancer. Pancreatic cancer models can be established either by inducing carcinogenesis or by implanting tumor cells or tissues into animals. However, a clear contradiction exists between the effectiveness of chemotherapy *in vitro*, current animal models and in the clinical setting. It appears that *in vitro* studies fail to represent the complex *in vivo* microenvironment.(47) Further understanding of the molecular basis of cancer development and progression requires the establishment of a microenvironment in experimental animals that closely mimic the human body.

1.4.1 Pancreatic Carcinogenesis Model

It is estimated that carcinogens induce 70% of human tumors. Specifically, many environmental factors are known to enhance pancreatic carcinogenesis as discussed previously.(44, 45) In a study by Pour et al., pancreatic cancer was induced using diidopropanolnitrosamine (DINP, 2,2-dihydroxy-di-N-propylnitrosamoine) in 100% of males Syrian golden hamsters and 90% the females.(48) Chester et al., has induced pancreatic adenocarcinoma *N*-nitrosobis(2-oxopropyl)amine (BOP) in 70 female Syrian hamsters.(49) BOP is used in the Syrian golden hamster and is known to produce pancreatic ductal adenocarcinomas that have similar histological characteristics to human tumors.(48) At the molecular level, mutations of K-*ras* at codons 12 and 13 have been reported to occur at a high frequency and at early stages in hamster tumors.(50)

Pancreatic cancer can be induced in rat model using a wide range of carcinogens. Dissin et al. were able to establish a pancreatic cancer model in rats by administering 7,12-dimethylbenz[a]anthracene (DMBA).(51) Induced tumors were a differentiated acinar phenotype which deviate from the ductal phenotype seen most commonly in human cancer.(52)

Mouse models have rarely been used in studies of pancreatic carcinogenesis. Most of the tumors induced in mouse models were acinar cell carcinomas. In a study by Osvaldt et al., 90 male CF-1 mice received DMBA implanted into the pancreas.(53) 47 mice developed pancreatic adenocarcinoma while 14 developed reactive hyperplasia. In other studies, Azaserine and M-methyl-N-nitrosourea have been used on Charles River CD-1 albino and C57BL/6J mice, respectively, and resulted in acinar cell tumors.(54) As in the rat model, most carcinomas show evidence of acinar differentiation.(52) Human

pancreatic ductal carcinoma is a very complex genetic disease and many aspects of it are poorly understood.(55) Despite advances in the technology to genetically develop mouse strains, transgenic mouse models fail to replicate human pancreatic cancer.(56)

1.4.2 Indirect Xenograft Model

Indirect xenograft models utilize established cell lines implanted into the organ of origin (orthotopic implantation) or into a different site (heterotopic implantation). Cell lines can be obtained from the American Culture Collection (ATCC).

The required cell mass for tumor engraftment and biological properties vary considerably depending on the cell lines and site of implantation. Cell lines should be carefully selected based on the objectives of individual research.(9) In a study by Morioka et al., the HaP-T1 cell line was established from chemically induced pancreatic cancer in Syrian golden hamsters, then implanted subcutaneously into Syrian golden hamsters (2×10^6cells/mL, 0.1 mL). Tumors were resected 4 weeks post-implantation and re-implanted into the pancreas at 1 mm^3 fragment per hamster. The control group of the same species received subcutaneous implantation of HaP-T1 cell line (2×10^6/mL, 0.05 mL).(57) The engraftment rate was 100% for both groups, however, local and distant metastases were significantly higher in the group receiving tumor tissue compared to control. A similar study has shown inconsistent results with inferior engraftment rates, local and distal metastasis.(58)

One of the early large, comprehensive studies by Marincola et al., MIA PaCa-2 cell line was implanted into 256 young and 92 adult male Swiss/NIH nude mice at 3 sites. The

orthotopic group (n=156) received (1 x 10^7 cells), the subcutaneous group received a similar dose (n=162) and a third group received intra-portal injection of a similar dose.(59) Operative mortality was 13.4% in the young population and 5.7% in adults. The engraftment rate for the subcutaneous group was 97.9% for young mice and 69.2% in the adult population. The growth rate was significantly higher in the young population. In the orthotopic group, the engraftment rate was 91.6% in young animals compared with adult animals which was 64.3%. Liver metastasis were significantly higher in the orthotopic group.(59) In a study by Mohammad et al., the pancreatic cancer cell line, HPAC, was injected directly into the pancreas of 5 week old SCID mice at 1 x 10^6 cells per transplant. All animals developed palpable tumors by 21 days post-injection (100% take rate).(60) In Alves et al., the human pancreatic ductal adenocarcinoma cell line (PancTu 1) was injected into the pancreas of SCID mouse model (n=21) and under the skin at a 1 x 10^6 cells per transplant (n=7). For the orthotopic group, 95% developed pancreatic adenocarcinoma in 4 weeks. For the heterotopic group, 100% developed pancreatic adenocarcinoma in 2-3 weeks.(61) In another study using the same cell line and concentration implanted orthotopically into 8 SCID mice, all mice developed pancreatic adenocarcinoma in 29 days.(62) A study by Trevino and colleagues used the pancreatic cancer cell line (L3.6pl) and implanted these cells in the pancreas of nude mice at doses of 1.25 x 10^5, 2.5 x 10^5 and 5 x 10^5 cells per transplnat.(63) All mice developed pancreatic cancer after 6 weeks. Heterotopic indirect xenograft models have been the most widely used mouse models for cancer research. It is relatively easy, reproducible and inexpensive when compared to orthotopic models. The subcutaneous model is easily accessible allowing for more accurate monitoring and assessment of

tumor growth and responses. However, the subcutaneous model rarely results in metastasis. Unfortunately, drugs that show very good activities against cancer in this model fail to show similar effect in patients.(7, 64) The orthotopic indirect xenograft mouse model is technically challenging, with increased risks of bleeding and even death. It is very expensive compared to the subcutaneous model with very little access to the transplanted cells. However, it provides a more natural microenvironment for implanted cells. Table 1-1 provides some of pancreatic cancer cell lines implanted into various animal models from the literature.

Table I: Some of the pancreatic cancer cell lines implanted into animal model in the literature

Cell line	Animal model	Number of implanted cells	Site of implantation	Sample size	Engraftment rate	Reference
MIA PaCa-2 (Pancreas)	Swiss/NIH nude mice	10 x 10^6 cells	Pancreas	135	80.7 % at 4 weeks	(59)
MIA PaCa-2 (Pancreas)	Swiss/NIH nude mice	10 x 10^6 cells	Subcutaneous	124	92 % at 2 weeks	(59)
HPAC (21)	ICR/SCID mice	1 x 10^6 cells	Pancreas	5	100 % at 3 weeks	(60)
PancTu 1 (Pancreas)	CB-17/Ztm SCID mice	1 x 10^6 cells	Pancreas	8	100 % at day 29	(62)
PancTu 1 (Pancreas)	SCID mice	1 x 10^6 cells	Pancreas	21	95 % in 4 weeks	(61)
PancTu 1 (Pancreas)	SCID mice	1 x 10^6 cells	Subcutaneous	7	100 % in 2-3 weeks	(61)
HaP-1 (Pancreas)	Syrian Golden Hamster	2 x 10^5 cells	Subcutaneous	16	100 % at day 7	(58)
AsPC-1 & MIAPaCa-2 (Pancrease)	SCID mice	1 x 10^6 cells	Pancreas	30	--	(66)
L3.6pl (Pancreas)	Nude mice (NCR-NU)	1.25 x 10^5 cells, 2.5 x 10^5 cells, 5 x 10^5 cells	Pancreas	20 22 23	100 % at 6 weeks 100 % at 6 weeks 100 % at 6 weeks	(63)

1.4.3 Direct Xenograft Model

Direct xenograft models utilize a freshly resected tumor fragments to be directly implanted into the organ of origin (orthotopic implantation) or a different site (heterotopic implantation). This approach minimizes the manipulation that could alter cancer properties. The tumor is transferred with its original stroma that allows for biological interaction between the tumor and the extracellular matrix leading to the development of a tumor of histological appearance similar to the original patient's tumor.(65) Preserving the microenvironment of the original tumor makes it more likely to behave similarly to the original human cancer. Therefore, if successfully performed, it can be an ideal model for studying tumor behavior and response to drug therapy. Multiple studies have indicated that direct xenograft models can reliably predict clinical responses in pediatric malignancies.(9, 66, 67) Production of metastasis depends on intrinsic properties of the tumor and the host microenvironment. An advantage of using direct xenografting is that all cellular fractions existing in the tumor will be implanted with the graft.(68, 69) Morioka et al. resected a pancreatic tumor aseptically from an indirect xenograft model (HaP-T1 cell line), minced the tissue into pieces of (1 mm^3) and implanted the tissue into the pancreas of Syrian golden hamsters (1 mm^3). A control group of the same species received an orthotopic implantation of HaP-T1 cell line (2×10^6/mL, 0.05 mL). The engraftment rate was 100% for both groups. However, local and distant metastases were significantly higher in the group that received direct xenograft compared to control.(70) In a study by Fu et al., nude mice nu/nu were used as a direct xenograft model for pancreatic cancer. Pancreatic cancers from surgical specimens of 5

individual patients were cut into 1 mm^3 pieces and subsequently attached to the pancreas of nude mice using 8-0 surgical sutures.(71) 15 of 17 mice developed pancreatic cancer with extensive local growth. Four of the five cases exhibited lymph node and distant metastasis.(71) Jimeno and colleagues utilized a direct xenograft model by successfully implanting a patient-derived tumor sample into athymic nude mice.(69) After engraftment, the tumor was resected and re-implanted for multiple generations to generate a cohort large enough for studying chemotherapy.(69) In a study by Farre et al., tumor tissue (10 mg fragments) of human pancreatic cancer were used for implantation into the pancreas, liver, colon and under the skin of nude mouse model. Differences in tumor behavior and metastasis were observed with different sites.(72) Table 1-2 is a comparison between orthotopic and heterotopic sites of implantation.

Table 1-2: Comparison between different sites of implantation xenograft

	Orthotropic site	Heterotopic
Implantation	Challenging	Relatively easy
Mortality	High operative risk	Minimal risk
Invasion/Metastasis	High	Rare metastasis < 2 %
Monitoring	Imaging, very large palpable tumor	Relatively easy, more accurate.
Study purpose	Tumor behavior and characteristics	Drug therapy

1.5 Animal Selection for Cancer Xenografts

The Syrian golden hamster is one of the first models used for pancreatic xenografting.(58, 73) Tumors induced in hamsters are very similar to those in humans in almost every aspect as discussed previously.(57) However, the hamster is immunocompetent, thus requiring relatively higher inoculum. In contrast, mouse models are widely available, less expensive with many immunodeficient strains, making them a popular option for tumor xenografting. Induction of pancreatic cancer in rats can be achieved with a wide variety of chemical agents.(52) However, most tumors in rat models tend to differentiate to acinar carcinoma, while ductal carcinoma is the most common type in human(52, 74).

Athymic nude mouse models have been widely used with excellent engraftment rates.(71) While they lack cell-mediated immunity (T-cell), athymic mice possess natural killer and defective humoral immunity. The absence of fur facilitates monitoring and assessment of tumor growth. This mouse model is widely available and relatively inexpensive. However, such a model can potentially modify tumor behavior since it is not completely immunocompromised. The severe combined immunodeficiency (SCID) mouse model is deficient in both T-cells and B-cells. It requires an even lower cell inoculum and more likely to exert less selection on the implanted tumor.(60, 61) Many studies have shown excellent engraftment rates for orthotopic and heterotopic sites of implantation. However, this model can develop infections easily, which can significantly alter tumor study outcomes. Non-obese diabetic NOD/SCID-gamma mice are deficient in T-cells, B-cells and natural killers, making them ideal candidates for direct xenografts.(9) However, they require extensive care due to severe immunodeficiency (Table 1-3)

Table 1-3: Summary of commonly used animals for xenotransplantation

	Immunodeficiency	Advantages	reference
Syrian golden hamster	Immunocompetent	Closely resemble human cancer.	(58, 73)
Rat	Variable	------	(52, 74)
Nude mice	Cell-mediated	Widely available, ideal for indirect xenograft	(59)
SCID mice	Cell-mediated and humoral		(60, 61)
NOD/SCID-gamma (NSG) mice	Cell-mediated, humoral and natural killer	Ideal for direct xenograft, require minimal inoculum	(9)

1.6 Conclusion

Pancreatic cancer is one of the most lethal diseases, whose etiology is yet to be understood. The 5-year survival rate is less than 14% for early stages of the disease. In humans, studying carcinogenesis and tumor behavior is extremely difficult, partly due to the relatively lower incidence rate of the disease. Prevention of pancreatic cancer is highly desired, however, randomized control trials are almost impossible in humans for that purpose. To date, prognostic biomarkers have yet to be developed. Most animal models currently employed are indirect xenografts, established from cell lines, and they frequently fail to predict drug response in the clinic. The extensive processing of cell lines and cryopreservation devoid the tumor from surrounding extracellular matrix and increases the chances for genetic mutations. Direct xenograft animal model has the potential to reliablly represent the clinical disease. In a recent report, a remarkable clinical outcome was achieved for a patient with pancreatic cancer who received chemotherapy guided by a direct patient-derived xenograft.(75) Such a personalized medicine approach has prolonged the patient's survival for over 55 months.(75) However, direct xenograft models are more challenging in terms of scarcity of tissue samples and the lower rates of engraftment. NOD/SCID-gamma (NSG) mouse model is ideal for this approach due to its deficiency in cellular, humoral and natural killer immunity. Direct implantation of tumor tissues into the pancreas carries significant morbidity and mortality risks. However, it has been shown that tumor behavior is more similar in terms of local and distant metastases, making it ideal for studying tumor behavior and detecting various biomarkers that can potentially contribute to early detection of the disease. Direct implantation of tumor tissue under the skin is relatively

easy with minimal morbidity and mortality rates. One huge advantage of this model is that the tumor is easily accessible so that the tumor size can be monitored precisely. The choice of animal model depends on the primary purpose of the study. Direct xenograft models, if utilized appropriately, can potentially predict the clinical behavior of individual tumor so that the most effective treatment is selected based on tumor response in the personalized mouse xenograft.

Chapter 2

Prevascularization of the Subcutaneous Space with a 'Device-Less' Technique Facilitates Human Pancreatic Cancer Engraftment and Growth in Mice

2.1 Introduction

Pancreatic cancer is the fourth leading cause of cancer-related death, with approximately 48,000 new cases occurring every year in the United States.(76) Despite the average lifetime risk of developing pancreatic cancer of 1.5%(76), the overall survival rate is less than 5% with an average survival duration of 4 to 6 months from the time of diagnosis.(6) The precise etiology of the disease has yet to be fully elucidated, however, smoking, diabetes mellitus, obesity, chronic pancreatitis, heavy alcohol consumption and a family history of pancreatic cancer have been linked to the development of pancreatic cancer.(17, 77) Surgical resection is currently the only treatment option offering a means to potentially cure the disease, although the 5-year survival rate is only 20% for stage 1 disease. (78) Moreover, less than 15% of the tumors are resectable at time of the diagnosis.(5) Together these factors contribute to the increasing interest to better understand the biology and control of pancreatic cancer.

Historically, animal cancer models have provided considerable insights into human cancer behavior and have contributed to the development and clinical use of effective chemotherapeutic agents.(79, 80) As such, the use of animal models has the potential to improve our understanding of pancreatic cancer and may lead to therapeutic interventions that could improve its prognosis. Pancreatic cancer has been successfully induced in a

Syrian golden hamster model using diisopropanolnitrosamine (DIPN) and N-nitrosobis (2-oxopropyl)-amine (BOP).(48, 49) However, carcinogenesis models are time consuming, as it takes an approximate average of 6 months for tumor development, with variable success rates.(51) Moreover, the resulting tumors have variable, poorly predictable phenotypes making them less relevant to the clinical manifestation of the disease.(51) For these reasons, xenograft animal models have been utilized to investigate human cancer biology. In this model, human cell lines that carrying a wide range of cancer genetics and phenotypes are implanted into immunodeficient mice.(58-63, 67) However, there is considerable variation in the required cell implant number for successful engraftment. For instance, a cell injection range of 0.5×10^6 to 10×10^6 cells has been reported to establish a palpable tumor for pancreatic cancer cell lines L3.6pl, Panc-1 and MIA-PaCa-2.(59, 63, 81-83) Several strategies have been developed to improve cell engraftment rates including the use of recombinant growth factors and co-implanting cell lines with liquefied basement membrane such as matrigel.(84-87)

In the present study, we investigate a novel subcutaneous implantation site for pancreatic cancer growth. This technique, recently developed in our laboratory for cell therapy(88), transforms the hypoxic subcutaneous tissue into a prevascularized space by temporarily implanting a medically approved angio-catheter for 4 – 6 weeks. Subsequently, upon removal of the catheter, a pancreatic cancer cell line is infused into the newly vascularized space. We hypothesize that this prevascularized space will improve cellular engraftment and enhance tumor growth.

2.2 Materials and Methods

2.2.1 Animals

Adult immunodeficient NOD.Cg-Prkdc^{scid}Il2rg ^{tm1Wjl}lSzJ (Jackson Laboratories, Bar Harbor, ME, USA) mice, herein referred to as NOD-scid gamma (NSG), 12-14 weeks of age were used. Animals were housed in a noro virus negative environment and all procedures were performed in a biosafety cabinet. All experimental procedures were approved by the University of Alberta Research Ethics and Animal Use Committee.

2.2.2 Creation of a Device-Less "DL" Subcutaneous Site

The DL site was created according to previously published methodology.(88) Briefly, a 1.5-cm segment of a 5-French nylon radiopaque angio-catheter (Torcon NB Advantage Beacon tip Cook Medical, IN, USA) was implanted subcutaneously in the right flank of NSG mice (Fig. 2-1a) through a 5 mm transverse incision using sterile micro-scissors. A small subcutaneous pocket was created by inserting the scissor tips through the incision with a gentle spreading motion before implanting the angio-catheter. The angio-catheter was removed 4-6 weeks, after a period of accelerated pre-implantation neovascularization, and tumors implanted into the modified space (Fig. 2-1b).

2.2.3 Proinflammatory Cytokine Analysis

To evaluate cytokine profiles in NSG mice, 1.5 cm segments of the angio-catheter were implanted for 24 h, 1 week, 2 weeks or 3 weeks (n=3 for each time point). The respective

area of non-implanted mice of the same strain and age were retrieved as baseline control (n=3). After removing catheters from specimens, samples were placed in pre-weighed microcentrifuge tubes to calculate tissue weights, and subsequently snap frozen with liquid nitrogen and stored at -80°C. Each tissue sample was homogenized (PowerGen, Fisher Scientific, Ontario, Canada) on ice for 30 seconds (x2) in1 ml of lysis buffer (0.15 M NaCl, 1 mM Tris-HCl, 0.1% SDS, 0.1% Triton X-100, 20 mM sodium deoxycholate, 5 mM EDTA) per 200 mg of tissue. Samples were then sonicated (VirSonic, VirTis, NY, USA) on ice with 10 quick pulses for 10 seconds. Lysed tissue samples were centrifuged at 400 g for 10 min at (4°C), then supernatant was collected and placed in microcentrifuge tubes to which 10 µL (1:100) of protease inhibitor cocktail (Sigma-Aldrich Canada Co., Oakvile, ON, Canada) was added. IL-1β, IL-6, IL-10, IL-12p70, KC/GRO and TNF-α were measured using a Multi-Spot Mouse ProInflamatory 7-Plex kit (Meso Scale Discovery, Gaithersburg, MD, USA) requiring 25 µL of lysate in triplicates and analyzed on a SECTOR Imager (Meso Scale Discovery, Gaithersburg, MD, USA).

2.2.4 Cell Culture

Human pancreatic carcinoma MIA-PaCa-2 (ATCC® CRL-1420, Manassas, VA, USA) and PANC-1 (ATCC® CRL-1469, Manassas, VA, USA) cell lines were obtained from American Type Culture Collection (ATCC, Manassas, VA, USA). Cell lines were sent to DDC Medical (Fairfield, OH, USA) to verify their authenticity. Results showed that cell lines matched the ATCC panel of markers. Cells were maintained in DMEM (ATCC, Manassas, VA, USA) medium supplemented with 10% fetal bovine serum, 100 U/ml penicillin-G and 100 µg/ml streptomycin (Sigma Aldrich Canada Co., Oakville, ON,

CA). All cultures were kept at 37°C with 5% CO_2 and subcultured at 2 to 3 day intervals to maintain exponential growth.

2.2.5 Tumor Implantation

Adherent pancreatic cancer cells, of both cell types were retrieved at > 70% confluence and washed with pre-warmed, sterile PBS using 2 ml of trypsin-EDTA (0.05% (vol/vol), Sigma Aldrich Canada Co., Oakville, ON, CA), then resuspended in a 50 ml centrifuge tube at 1 x 10^6 cells per ml (viability > 95% by trypan blue (0.4%) exclusion, Sigma Aldrich Canada Co., Oakville, ON, CA) of the culture medium descried above. The cell suspension was centrifuged again at 300 g at room temperature for 5 min then cells were resuspended in 20 ml of sterile HBSS (Corning-cellgro, Manassas, VA, USA) containing 1% (vol/vol) serum free Matrigel Basement Membrane Matrix (BD Biosciences, San Jose, CA, USA) maintained at 4°C at 10 x 10^6 cells/ml in order to bring the final cell inoculum to 1 x 10^6 cells per 100 μL. Then 100 μL of the suspension was aspirated using 1-ml syringes, capped with 23-gauge needles and placed immediately on ice. Mice received DL implantations on the right flank and conventional subcutaneous (SQ) implantation on the left flank. For DL implantation, a 5 mm incision was made cranial to the implanted catheter on the right flank under anesthesia. The tissue around the tip of the catheter was dissected to withdraw and remove the catheter. PE-50 tubing was carefully attached to the 23-gauge needles capping the syringes containing cell inoculums and delivered to the pre-vascularized lumen, with cells subsequently injected into the lumen. The incision was closed with a surgical staple (Autoclip, Becton Dickinson, Sparks, MD, USA). For SQ implantation, the skin over the left flank was gently grasped with forceps

for counter-traction, the skin was penetrated while directing the needle parallel to the animal's body. Cells were then injected slowly and the needle subsequently withdrawn (Fig. 2-1 e & f). All mice then received 0.1 mg/kg subcutaneous bolus of buprenorphine (away from the transplant site) and monitored for 2 min for gross leakage.

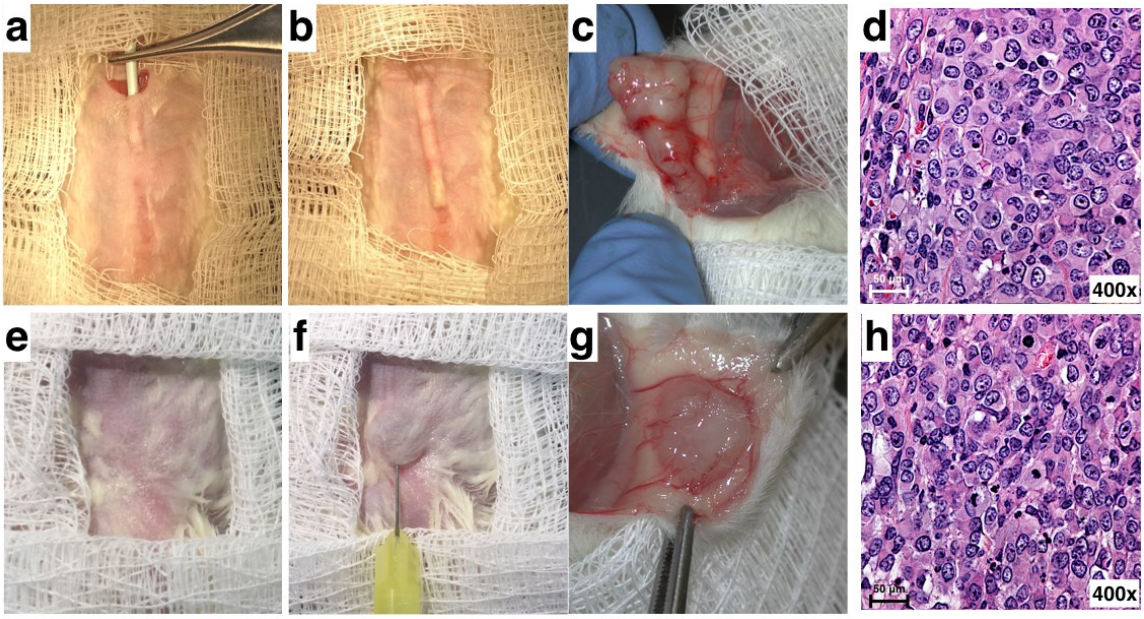

Fig 2-1. The "deviceless' technique vs. conventional subcutaneous method. (a) A medically approved angio-catheter is temporarily implanted under the skin to be removed 4-6 weeks later (b) after maturation of the site. (c) Gross appearance of MIA-PaCa-2 cell line generated tumor at the DL site 6 weeks post transplantation. (e) Unmodified subcutaneous site to which MIA-PaCa-2 cell line suspension is injected (f) by the conventional subcutaneous inoculation method. (g) Gross appearance of MIA-PaCa-2 cell line generated tumor at the SQ site 6 weeks post transplantation. (d) The histological appearance of MIA-PaCa-2 cell line implanted into the DL site appeared similar to same cell line implanted into the SQ site (h).

2.2.6 Evaluation of Tumor Growth

Mice were monitored twice a week for tumor volume and general health. Tumor measurements were obtained using a manual caliper. Tumor volume was calculated using the formula: Tumor volume = $(\text{width})^2$ x (length)/2.(89)

2.2.7 Histological Assessment

All tumors were resected 63 days after implantation before euthanasia and kept in formalin (Fig. 2-1 c & g). Samples were impeded in paraffin and slides were stained with Hematoxylin/Eosin and Masson's trichrome. DL sites were also created in a group of NSG mice then DL sites were explanted 4 weeks after implantation to assess vascularization. Immunofluorescence staining was performed using primary antibody of rabbit anti-CD31 (1:50; abcam, Cambridge, MA, USA) overnight at 4 °C. Secondary antibody of goat anti-rabbit (1:200; Fluorescein, Vector Laboratories, Burlingame, CA, USA) were used on the second day of staining. Samples were counterstained with DAPI anti-fade mounting medium (ProLong, LifeTechnologies, Eugene, OR, USA). Slides were examined under fluorescent microscopy and photographed using the appropriate filter with AxioVision imaging software.

2.2.8 Statistical Analysis

Tumor volume and proinflammatory cytokine data are presented as mean ± SEM. The differences between groups for proinflammatory cytokine data were calculated using one-way ANOVA with Tukey's post-hoc tests. The average tumor volume for the DL and SQ

groups were calculated and compared using 2way ANOVA with Bonferroni's multiple comparison test. All statistical analyses were conducted using GraphPad Prism (GraphPad Software, La Jolla, CA, USA). $P< 0.05$ was considered significant.

2.3 Results

2.3.1 Creation of a Prevascularized DL Site Accelerated Tumor Growth in NSG Mice

To test the efficacy of the DL technique, NSG mice were implanted with MIA-PaCa-2 or PANC-1 cell lines. Animals received $1x10^6$ cells DL implant on the right flank and $1x10^6$ cells SQ implant on the left flank. For MIA-PaCa-2 cell line (n=17), the average tumor volumes were larger in the DL site at all time points compared to the SQ site. This difference was statistically significant 60 days after implantation with the greatest tumor volume at the time of euthanasia (1943 ± 598 vs. 643.8 ± 116.3 mm^3, $P< 0.05$, respectively) (Fig. 2-2 a). Similarly, the average tumor volumes were larger in the DL group compared to SQ group for the PANC-1 cell line (n=16). However, this difference was not statistically significant with the greatest tumor volume at the time of euthanasia (419.8 ± 54.13 vs. 268.4 ± 65.25 mm^3, respectively) (Fig. 2-2 b). The engraftment rate was 100% for both cell lines at all sites. The resulting tumors from both cell lines showed a similar histological appearance in the DL site as compared to the SQ site (Fig. 2-1 d & h).

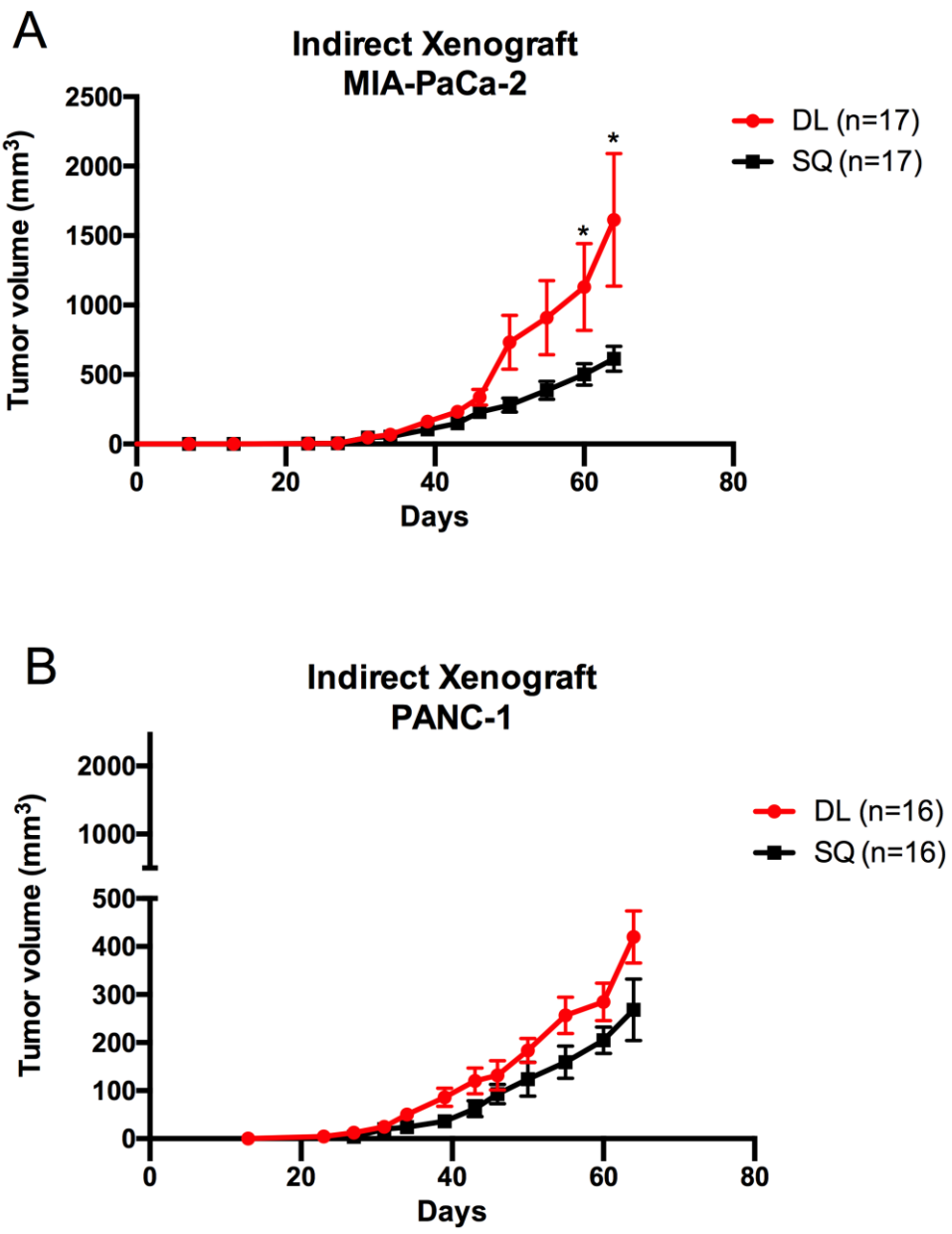

Fig 2-2. Tumor volume measurement obtained using the formula: Tumor Volume = (Width)^2 x Length/2. (a) NSG mice implanted with MIA-PaCa-2 cell line using the DL method on the right flank vs. SQ implants on the left flank (n=17). (b) NSG mice implanted with PANC-1 cell line following the same methodology (n=16). The average mean tumor volumes for each group were compared using 2way ANOVA with Bonferroni's multiple comparison test. $P<0.05$ considered significant.

2.3.2 NSG Mice have a Robust Inflammatory Reaction to the Implanted Angio-catheter

We observed a strong cytokine and chemokine response elicited by the implanted angio-catheter (Fig. 2-3). Interleukin (IL-) IL-1β, IL-6 and IL-12p70 reached their peak at 24 h after implantation and were significantly higher than non-implanted controls ($p<0.0001$, One-way ANOVA with Tukey's post-hoc test) (Fig. 3a-b and f). In contrast, IL-10, tumor necrosis factor α (TNF-α) and keratinocyte growth factor (KC/GRO) reached their peak one week after implantation and were significantly higher the control ($p<0.0001$,$p<0.0001$ and $p<0.05$ respectively, One-way ANOVA Tukey's post-hoc test) (Fig. 2-3 c-e). However, the inflammatory response was alleviated and all cytokines levels were similar to control by 2 weeks after implantation ($p>0.05$, student'st-test) (Fig. 2-3 a-f).

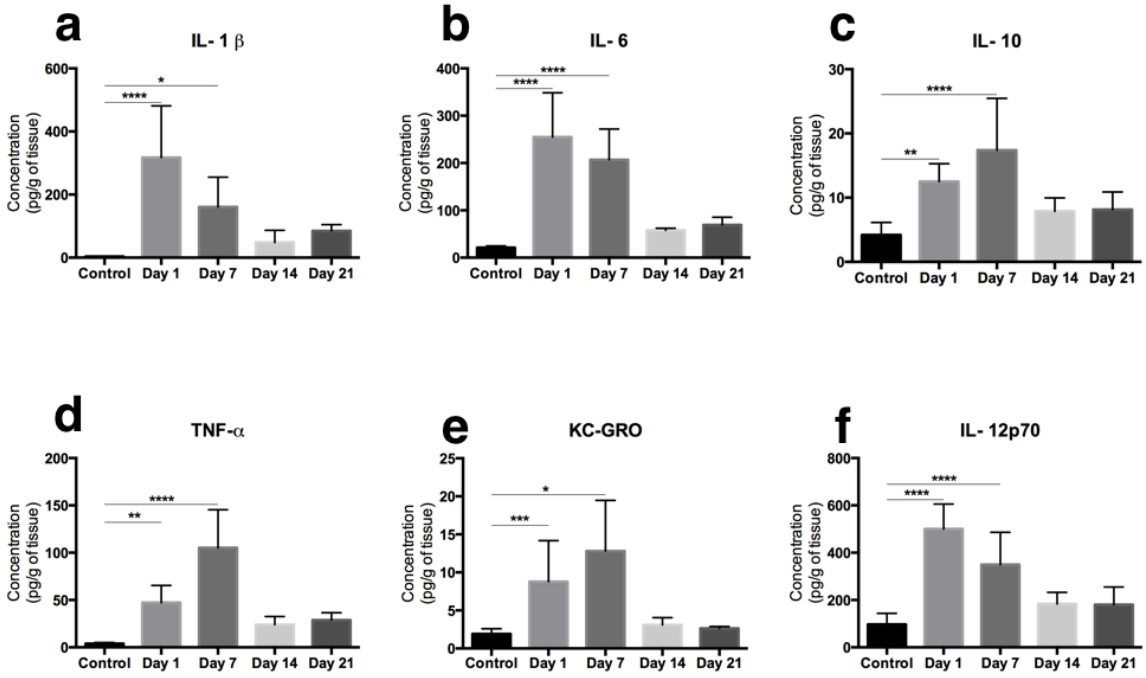

Fig 2-3. The transient inflammatory response to the implanted angio-catheter 24 h, 7 days, 14 days and 21 days post-implantation as indicated by the proinflammatory markers profile. (a-f) The proinflammatory concentrations of IL-1β, IL-6, IL-10, IL-12p70, KC/GRO and TNF-α. Data are presented as mean ± SEM for pg/g of tissue. *P<0.05, **P<0.01, ***P<0.001, ****P<0.001 (n=3/time point). Comparisons between concentrations at different time points were conducted through one-way ANOVA with Tukey's post-hoc test.

2.3.3 DL Increased Vascular Density

DL sites were explanted 4 weeks after transplantation (n=3) in addition to the unmodified subcutaneous space (n=3). Gross assessment of the DL site revealed dense vascular networks. Histological analysis of explanted DL sites (non-tumor bearing) showed a hollow void space surrounded by a connective tissue capsule (Fig. 2-4 a-b) rich in blood vessels compared to unmodified subcutaneous space (Fig. 2-4 c-d). Similarly, the explanted DL site of PANC-1 cell line tumor implant, one week after implantation, showed a tumor graft surrounded by a dense, vascularized connective tissue capsule (Fig. 2-4 e-f).

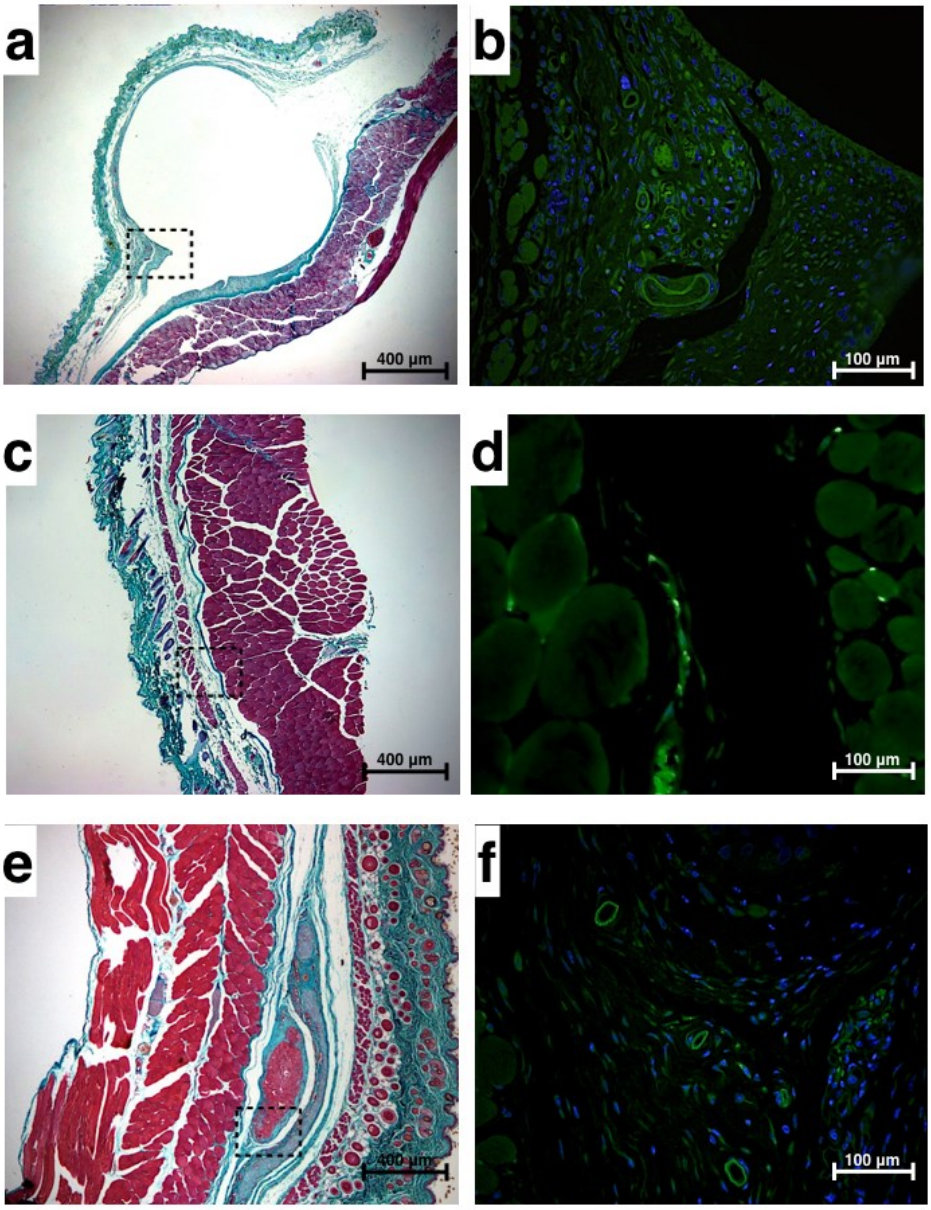

Fig 2-4. Histological analysis of the implantation DL site. (a) A representative cross-section of Masson's trichrome stained DL site (non-tumor bearing) after removal of the catheter that had been implanted for 4 weeks at low magnification (20x). Collagen (blue), smooth muscle (red). (b) fluorescent staining of the same cross-section stained blood vessels (green) and nuclei (blue) at higher magnification (400x). (c) Masson's trichrome stained cross-section of naïve (unmodified site) at low magnification with fluorescent staining of the same section at higher magnification (d). (e) Masson's trichrome stained representative cross-section of PANC-1 cell line implanted into the DL site 1 week after implantation at (20x) showing the tumor graft (arrow) surrounded by connective tissue capsule. (f) Fluorescent staining of the same section showing multiple blood vessels at higher magnification (400x).

2.4 Discussion

In the present study, we explored the utility of the novel DL technique(88), previously developed in our laboratory, to support cellular engraftment and growth of pancreatic cancer cells in an animal model. We postulated that the DL technique primes the subcutaneous site and generates conditions favorable for cellular implantation. In a previous report, the DL technique was superior to the conventional unmodified subcutaneous transplantation method as evidenced by the unprecedented reversal of diabetes in mice receiving subcutaneous DL pancreatic islet transplantation.(88) The beneficial effect of the DL technique is attributed to the development of fibrovascular stroma without the need for a permanently implanted device.

The DL technique is designed to take advantage of the natural foreign body inflammatory reaction.(88) However, NSG mice used in the present study are immunocompromised. To evaluate the efficacy of the DL approach in this mouse model, we have measured proinflammatory markers at the DL site at different time points. A robust inflammatory reaction resulted from implanting the catheter as indicated by elevated proinflammatory cytokines after the first week of transplantation. However, levels of detected proinflammatory cytokines were similar to baseline control two weeks post-transplantation. Of note, the DL approach has reportedly enhanced islet engraftment in 3 different mouse models, including immunodeficient $Rag^{-/-}$ mice that have defective cell-mediated immunity similar to NSG mice.(88) Our results indicate that NSG mouse model is indeed suitable for this approach. Prompt removal of the catheter 4 to 6 weeks after transplantation, when a vascularized collagen network has developed, further ensures the cessation of inflammation and negates fibrosis at the site of implantation.

We proceeded then to test the DL technique with pancreatic cancer cell lines. As anticipated, we have observed accelerated tumor growth in both MIA-PaCa-2 and PANC-1 cell lines in the DL site. The observed effect of the DL approach is likely to be mediated by the increased vascular density at the DL site, prospectively facilitating oxygen and nutrient delivery to the xenograft. The vascular density at the DL site was previously quantified by Pepper et al., and was found to be significantly higher than the unmodified subcutaneous space.(88) The beneficial effect could also be attributed to the development of a stromal bed induced by the transient inflammatory reaction. It has become recognized that the stroma plays an important role in tumor growth and development.(65) In previous reports, a humanized stromal bed was created by implanting human fibroblasts two weeks prior to cancer xenograft and resulted in successful engraftment of human squamous cell carcinoma and breast cancer.(90) (91) We have observed in our histological assessment a vascularized collagen matrix capsule in the explanted grafts 4 weeks after implantation. We did not observe any morphological differences between grafts from the DL site as compared to SQ site for both cell lines. In a study by Patel and colleagues, a glass disc or Gelfoam core was implanted subcutaneously 2 weeks prior to tumor xenograft in athymic nude mice.(91) Successful engraftment of 22 different human squamous cell carcinomas was achieved, which previously failed in the conventional, unmodified subcutaneous method.(91) While the newly developed stromal bed was not characterized in their approach, the outcomes were consistent with our results. Interestingly, the results reported by Patel et al. were not reproducible in NOD-SCID mice, which was attributed to the severity of immunodeficiency in this mouse model.(91) However, we have previously established

that the inflammatory reaction significantly varied based on the implanted catheter material, diameter and duration of implantation.(88)

In ongoing studies, we are actively capitalizing on the DL approach to facilitate patient-derived tumor xenograft (PDX) models in a personalized medicine approach, where fresh tumors are implanted directly into immunodeficient mice within hours of resection without modification.(9, 11, 69, 92-95) One of the major advantages of PDX, when successful, is that the resulting tumors preserve the original histology and tumor marker expression making it more clinically relevant.(11) The DL approach has the potential to accelerate tumor growth and reduce the required tumor load for engraftment. It is estimated that 85% of new drugs, that were promising in animal studies, fail in early clinical trials.(96) In a recent promising pilot clinical study utilizing PDX guided treatment, one patient died before receiving the treatment.(10) Typically, multiple passages of tumor is required to generate sufficient tumor tissue due to limited access to PDX.(97) The DL approach has the potential to shorten tumor growth time to make it available for testing.

In conclusion, we report a simple and reliable cancer xenograft model utilizing the DL approach. In this approach, we modified the local graft microenvironment, generating favorable conditions for cellular implantation, by inducing a transient inflammatory reaction, leading to the development of a vascularized stromal bed. This approach can potentially be useful for cancer cell lines that are difficult to grow. It can also be implemented in PDX model in personalized medicine to take advantage of the accelerated tumor growth making it available for testing. Although we do not anticipate

major limitations of this approach in the PDX model, this remains to be tested in our current pancreatic cancer PDX studies at the University of Alberta.

Chapter 3

Applications of Mouse Xenograft in Cancer Therapy

3.1 Introduction

Animal cancer models have provided considerable insights into cancer behavior and contributed significantly to the development and clinical use of many chemotherapeutic agents.(79, 80) In this chapter we discuss our experience with the cancer direct xenograft mouse model and its clinical significance. We have conducted a preliminary study to test the feasibility of using the prevascularized DL subcutaneous site in this model. Solid tumors generated from pancreatic cancer cell lines were initially used. We then moved toward utilizing patient drive xenograft (PDX) in NSG mice. We will discuss the clinical significance of utilizing this approach, discuss obstacles associated with PDX and provide potential solutions.

We will also discuss a potential drug-drug interaction between tyrosine kinase inhibitors and nucleoside analogues for chemotherapy. Gemcitabine plus erlotinib combination is an FDA approved treatment for pancreatic cancer.(98) However, a recent *in vitro* analysis suggested that tyrosine kinase inhibitors may reduce the activity of gemcitabine by denying it access to the cell.(99) In this chapter, we explore the mechanism by which tyrosine kinase inhibitors can potentially prevent gemcitabine, the first line of treatment for pancreatic cancer, from entering the cell and we propose an *in vivo* study to further assess the extent of this potential interaction.

3.2 Mouse Xenograft in Personalized Cancer Medicine

3.2.1 Background

The current model for drug testing relies on implanting well-established cell lines which have adapted to *in vitro* growth.(97) Despite the success in treatment of certain cancers, such models have severely restricted ability to predict tumor responses to drugs in the clinic.(7, 97) In fact, only 15 % of novel drugs survive phase-I clinical trial evaluation despite successful pre-clinical testing.(7, 8, 96) It is estimated that only one in five cancer clinical trials is published, mainly due to failure to meet positive endpoints.(100) The multiple passages and cryopreservation of cell lines have the potential to alter cellular and molecular biomarkers and increase the chances of genetic mutations. Moreover, the process of enzymatic cell dissociation devoid the tumor from its original stroma, which has a significant impact on tumor behavior.(101) The interaction between cancer cells and their surrounding stroma has been proven to be essential for certain types of cancers such as squamous cell carcinoma.(65, 90, 91)

The lack of clinically relevant mouse models has shifted the interest of many researchers to utilize a PDX model.(9, 10, 69, 95, 97, 102) In this approach, also referred to as a direct xenograft model, a freshly resected tumor is implanted into immunodeficient animals without modification.(9) By doing so, the tumor is implanted with a considerable amount of its original stroma and potentially its associated signaling molecules. Analysis of cancer growth and infiltration, as well as histopathological assessment, including gene expression and biological markers can be conducted for that specific tumor. Multiple studies in the literature have shown preservation of PDX morphology with no change of

cytokines and gene expression.(10, 11, 103, 104) Such a personalized xenograft model allows for selecting the most effective therapy for an individual patient. In a recent report, a remarkable clinical outcome was achieved for a patient with advanced, infiltrating ductal adenocarcinoma who failed treatment with gemcitabine, a standard therapy, and treated with mitomycin C based on its response against the patient's personalized xenograft.(75) This treatment resulted in a long (50+ months) tumor response after the addition of cisplatin, as compared to the average median survival of 6.7 months for gemcitabine alone.(75, 105) This promising development shows a strong correlation of the drug-response in a personalized xenograft and the patient. It would be of great clinical use to establish this model given the high potential to improve pancreatic cancer prognoses here at University of Alberta.

3.2.2 Mouse-derived Xenografts

In preparation of establishing a PDX model for pancreatic cancer, we have started a mouse-derived xenograft utilizing the tumors generated from MIA-PaCa-2 and PANC-1 cell lines to optimize our protocol. Freshly resected tumor fragments were implanted into NSG mice according to the previously published methodology by Kim et al,.(9) Briefly, resected tumors were washed 3 times in sterile RPMI-1640 culture media (Sigma Aldrich Canada Co., Oakville, ON, CA) with 1% (vol/vol) antibiotic (100 U/ml penicillin, 100 U/ml streptomycin, 0.25 µg/ml amphotericin B, Sigma Aldrich Canada Co., Oakville, ON, CA). Tumors then were minced into 1 mm^3 fragments, with each fragment equivalent to 1 x 10^5 cells.(9) Tumors were immersed in media and maintained on ice until transplantation approximately 30 minutes later. Each animal received 5 fragments subcutaneously (SQ) on the left flank and 5 fragments on the right flank as a DL implant.

The DL implantation was performed by manually introducing tumor fragments into the DL subcutaneous space using microforceps. All tumor fragments successfully engrafted for both MIA-PaCa-2 and PANC-1 generated tumors. We did not observe a difference in cancer growth rate between the two approaches for both tumor types. However, the time to engraftment was shorter for fresh mouse-derived xenografts compared to cell lines (Fig. 3-1). A possible explanation is that cell line-generated tumors have already incorporated into host tissue and established their own connective tissue stroma. By utilizing direct xenograft approach, the tumor is transferred with its original microenvironment and thus would have a higher chance of engraftment. (65) For that reason, we did not see a benefit for prevascularaziation. To the contrary, dissociated cell lines have shown significantly accelerated tumor growth when implanted into the prevascularized subcutaneous space (Fig. 3-1).

This experiment demonstrates the feasibility of utilizing the DL technique for solid tumor implantation. Furthermore, it has demonstrated that direct xenograft implantation, when successful, has an accelerated rate of growth. These observations are of great clinical value in the assessment of tumor biological markers, as well as conducting subsequent drug response analysis in time to predict the most appropriate treatment for a specific tumor.

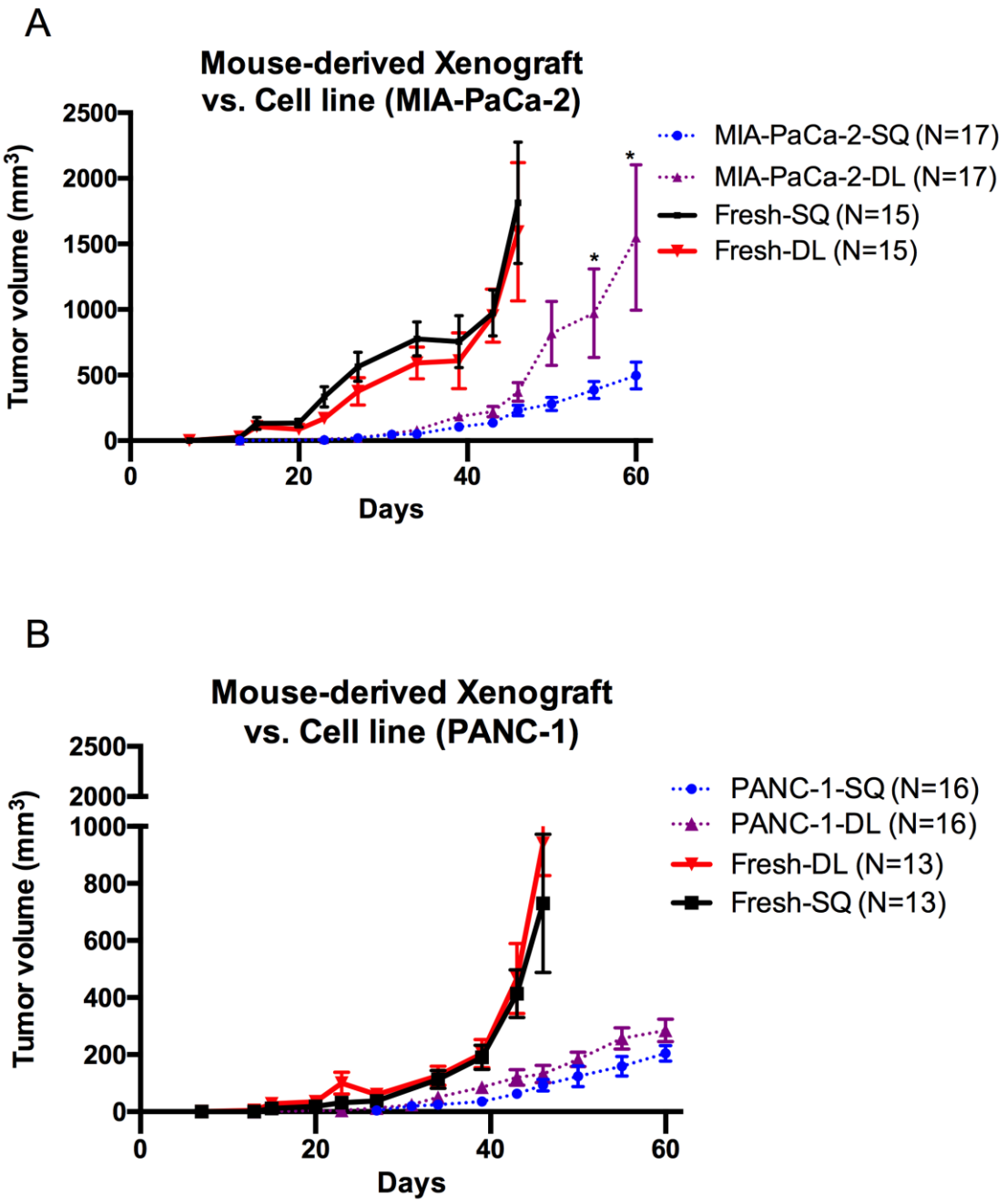

Fig 3-1. Cancer growth rates in mouse-derived xenograft compared to cell lines. (A) NSG mice implanted with the MIA-PaCa-2 cell line using the DL method on the right flank vs. SQ method on the left flank, compared to mouse-derived xenografts generated from fresh tumors, implanted in a similar fashion. (B) NSG mice implanted with PANC-1 cell line and PANC-1 generated fresh tumor following the same approach. Tumor volumes were calculated using the formula: tumor volume = $(\text{Width})^2$ x (Length)/2. The average mean tumor volumes for each group were compared using 2way ANOVA with Bonferroni's multiple comparison test. P<0,05 considered significant. Cell lines data (dotted lines) were obtained from chapter 2, which is under review at *Pancreas* journal.

3.2.3 Patient-derived Xenografts

All work was approved through the Health Research Ethics Board of the University of Alberta (HREB, Study ID# Pro00045315). Informed consent was obtained from 7 patients with pancreatic cancer to be enrolled in the study. Samples were obtained from 3 of the 7 patients. The remaining 4 patients were found to have unresectible tumors at the time of surgery. For the first 2 patients assessed, tumor samples were obtained from liver lesions suspected of metastasis. Fresh tumor fragments were implanted into 2 NSG mice per specimen. Each animal received a SQ implant on the left flank and DL implant on the right flank. The third patient was diagnosed with a neuroendocrine tumor (insulinoma) and multiple biopsies were obtained from the tumor after surgical resection. Fresh tumor fragments were implanted into 5 NSG mice on the right flank into the DL site and 4 NSG mice on the left flank into the SQ site. Tumor implantation was conducted following the approach mentioned previously.(9)

Unfortunately, the implanted tumors did not successfully engraft after following the mice for more than 8 weeks. One possible explanation is the extensive desmoplatsic reaction, which is a hallmark of pancreatic cancer, and its interference with selecting appropriate tumor samples.(106, 107) Pancreatic cancer is known to induce a significant amount of fibrosis, making it virtually impossible to differentiate between actual tumor tissue and fibrosis without microscopic examination since both exhibit firm-to-hard consistencies. In the clinical setting, the priority is to accurately establish the pathological diagnosis and staging. Excisional biopsy, which is ideal for implantation, is not feasible because it changes tumor borders, therefore, compromising the ability to accurately stage the disease. Unlike mouse-derived xenografts, we are restricted to needle core biopsy,

which provides minimal amounts of tissue without cutting the tumor open. Due to the scarcity of the sample, microscopic examination is not possible and all obtained tissue is implanted without verification. One potential solution is to have a pathologist available in the operating room during resection, which can facilitate appropriate sample selection without compromising diagnosis.

Another possible explanation is prolonged ischemia time due to the nature of surgical resection. The Whipple procedure involves ligation of blood supply before resection, which could take hours.(108, 109) Taking a biopsy before resection is associated with a high risk of bleeding since pancreatic cancer is highly vascularized.(110) The high metabolic demands for cancer cells make them susceptible to ischemia, which could potentially compromise viability. Early planning for animal implantation helps minimizing the time to implantation, thus the effect of ischemia.

The successful engraftment rates for patient-derived xenografts, in general, is variable and may range as low as 20%.(9) We had access only to 3 tumor specimens for this experiment, which does not have enough power to properly assess this approach. In future studies, it would be interesting to increase the sample size taking into consideration the appropriate selection of tumor sample, limiting animal implantation to one mouse per sample and minimizing the time to implantation, which potentially increase the odds for successful engraftment. Furthermore, utilizing the DL technique in this setting can potentially improve the chances of successful engraftment.

3.3 Erlotinib May potentially Protect Cancer Cells from Gemcitabine Cytotoxicity by Inhibiting Human Nucleoside Transporters

3.3.1 Background

Before the introduction of gemcitabine about 20 years ago, fluorouracil-based thereby was the first line of treatment for pancreatic cancer with a median survival rate of 4.4 months in advanced or metastatic disease.(5, 111) Today, the overall 5 year survival rate is only 7.2 % in the United States.(112) Many agents have been tested for the treatment of pancreatic cancer including FOLFIRINOX (oxaliplatin, irinotecan, leucovorin and fluorouracil) erlotinib, axitinib and *nab-paclitaxel*.(105, 113-115) However, gemcitabine is still considered the first line of treatment as a single agent due to its relatively low side effects profile.(114) The average overall survival for gemcitabine as a single therapy ranges between 4.8 to 13 months within the last 20 years.(105, 113-117) Gemcitabine is a pyrimidine nucleoside analogue that gains access to the cell via nucleoside transporters across plasma membrane. It incorporates into the DNA of rapidly dividing cells and prevents the DNA polymerases from adding more deoxynucleotides and results in cell death.(117, 118) Gemcitabine enters the cell mainly via the human equilibrative nucleoside transporter (hENT-1), which can be functionally inhibited by nitrobenzylmercaptopurine ribonucleoside (NBMPR-p).(99, 117, 119, 120) Spratlin et al. has shown that the absence of hENT-1 in immunohistochemistry was associated with a significant reduction in median survival time (13 vs. 4 months) of patients treated with gemcitabine alone for pancreatic adenocarcinoma.(117) In a phase-III clinical trial, the

combination treatment of erlotinib with gemcitabine for pancreatic cancer was shown to significantly prolong survival by two weeks.(113) However tyrosine kinase inhibitors, including erlotinib, inhibited hENT-1 *in vitro* in a recent report.(99) This could potentially protect cancer cells from gemcitabine cytotoxicity by inhibiting hENT-1. It would be of great clinical value to study the interaction between these two drugs in an animal model. One possible way to evaluate the activity of gemcitabine *in vivo* is to use a positron emission tomography (PET) tracer with 3`-deoxy-3`-fluorothymidine ([18F]FLT), which was previously shown to access the cells via hENT-1, the same nucleoside transporter as gemcitabine.(121) In an ongoing study in our laboratory, we sought to further explore this interaction in a mouse model by measuring [18F]FLT uptake in the presence and absence of erlotinib, as well as NBMPR-p as a positive control.(99, 120)

3.3.2 Study Design and Preliminary Results

All experimental procedures were approved by the University of Alberta Research Ethics and Animal Use Committee. The MIA-PaCa-2 cell line, which expresses hENT-1(120), was implanted into NSG mice on the dorsal surface, above the right shoulder following the methodology descried in Chapter 2 for subcutaneous implantation. After the tumor reached approximately 10 x 10 mm^2 6 weeks after implantation, animals were divided into 3 groups: one group received erlotinib at10 mg/kg in 6% captisol, IP for 3 days (N=6), another group received NBMPR-p at 15 mg/kg in 6% captisol, IP for 3 days (N=6) and the control group received 6% captisol, IP (N=6). All mice were scanned with PET tracer for one hour after receiving [^{18}F] FLT, representing gemcitabine treatment (Fig. 3-2).

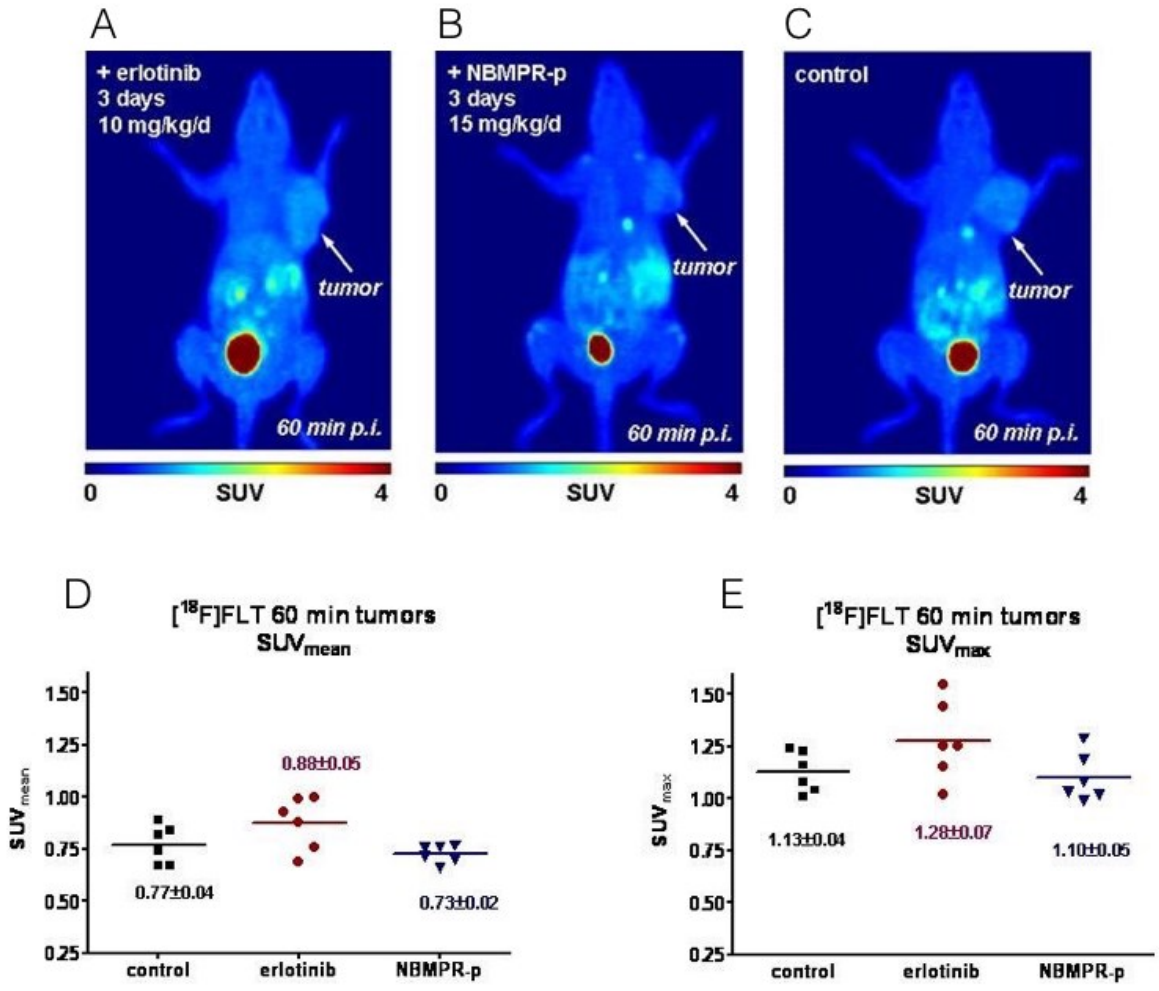

Fig 3-2. [^{18}F]FLT uptake measured by PET scanner. (A, B and C) are representative images of the three study groups showing tumors above the right shoulder (arrows). (D) [^{18}F]FLT mean uptake and maximum uptake (E) during the 60 min of PET scanning.

Surprisingly, [^{18}F]FLT uptake was similar in all three groups. We did not see a significant reduction in [^{18}F]FLT for the NBMPR-p group, which indicates a sub-therapeutic concentration at the time of imaging. This could be explained by the short half-life of NBMPR-p, which is about 45 minutes. NBMPR-p inhibited the nucleoside transporter *in vitro* at 1mM concentration(120). However, there is insufficient data for NBMPR-p use *in vivo* and 15 mg/kg could possibly be a suboptimal dose. NBMPR-p was given an hour prior to imaging. It may be beneficial to administer the drug immediately prior to imaging to determine if different results would be obtained.

Interestingly, we did not see a reduction in [^{18}F]FLT uptake as well in the erlotinib treatment group when using the prescribed 10 mg/kg dose. These outcomes were not expected as erlotinib inhibited hENT-1 in culture which should reduce [^{18}F]FLT uptake by cancer cells.(99) Again, this suggests a suboptimal tissue concentrating at the time of imaging. We chose 10 mg/kg based on the clinical recommended daily dose of 150 mg. However, differences in metabolism and clearance in mice vs. humans may require the use of a higher dose in mice. Of note, erlotinib was given for 3 days only, including the day of imaging, to help minimize the cytotoxic effect of erlotinib on cancer cells. Erlotinib can decrease cancer cell metabolism and proliferation, which can be a confounding factor in the present study. We have collected tissue samples from the three study groups and plan to assess the tissue concentration of [^{18}F]FLT, erlotinib and NBMPR-p.

We plan to repeat the experiment with a higher dose of erlotinib (50 mg/kg) to be given intraperitoneally for 3 days. We also plan to administer NBMPR-p within 20 minutes of imaging intravenously or intraperitoneally and harvest blood and tissue samples

subsequent to imaging. If erlotinib is found to reduce the uptake of FLT, then it may be advisable to not administer erlotinib and gemcitabine simultaneously when treating pancreatic cancer. Also of note, FLT should not be used as a measure of proliferation in patients treated with tyrosine kinase inhibitors because it may give false negative results due to the inhibition of hENT-1.

Chapter 4

Lung-derived Microscaffolds Facilitate Diabetes Reversal after Mouse and Human Intraperitoneal Islet Transplantation

4.1 Introduction

Type 1 diabetes mellitus (T1DM) is a chronic autoimmune disorder characterized by destruction of pancreatic β-cells and insulin deficiency.(122, 123) Life-long exogenous insulin replacement remains standard management. While intensive insulin treatment delays microvascular complications, it significantly increases risk of severe hypoglycemic events that can be disabling and occasionally fatal.(124-126)

In the past decade, pancreatic islet transplantation has shown promising outcomes with 5-year insulin independence rates approaching 50% in selected centers.(127, 128) To date, intrahepatic islet infusion via the portal vein is the only clinically approved site that has routinely resulted in insulin independence.(128, 129) In spite of recent advancements in islet transplantation, up to 70% of transplanted islets fail to engraft within the early post-transplant period.(126, 130) A major contributor to initial loss is the innate instant blood-mediated inflammatory reaction (IBMIR), resulting from exposure of islets to blood.(131, 132) Identifying alternative sites for islet transplantation could potentially ameliorate this effect, thereby reducing islet loss. Furthermore, the process for islet isolation and purification disrupts islet vasculature and injures the local microenvironment, further compromising engraftment.(133, 134)

The islet microenvironment is composed of a peri-insular basement membrane (BM) and extracellular matrix (ECM).(135-137) The ECM is a complex of different molecules that serves as a physical site for attachment and support, as well as a framework for cellular proliferation, differentiation and communication.(135, 138-141) The ECM binds and stores many cytokines, growth factors and other signaling molecules that modulate cellular behavior.(137, 142) Loss of peri-insular BM and apoptosis are evident immediately after enzymatic islet digestion.(138-140) Collagen-IV, laminin and fibronectin are the most commonly reported components of this microenvironment.(137, 138) Multiple studies have shown enhanced *in vitro* islet function for islets co-cultured with ECM components including collagen-IV, fibronectin, laminin, thrombospondin and heparin sulfate.(143-147) Islets embedded within a collagen gel maintain their spherical structure and secretory capacity compared to islets cultured under standard conditions.(148) As demonstrated by Wang *et al*., the apoptotic index, was significantly higher for islets cultured in standard conditions compared to islets co-cultured with collagen or fibronectin.(138)

Although interaction between islets and their surroundings is complex and incompletely understood, supplementing transplanted islets with ECM components and restoring the three-dimensional (3D) architecture appears to have a beneficial effect as evidenced by improved viability and function. (149-152) Islets seeded on a poly(dimethylsilonxane) 3D scaffold, collagen matrix or fibroblast populated collagen matrix have shown improved *in vivo* function.(149-151) Salvay *et al.* seeded islets on microporous, biodegradable poly(lactide-co-glycolide) (PLGA) scaffolds coated with collagen-IV,

fibronectin or laminin and found that diabetic mice exhibited significantly shorter time to restore normoglycemia compared to controls.(152)

Recently, organ-derived microscaffolds have been prepared from decellularized lung tissue, engineered endocrine micro-pancreata (EMPs), and subsequently seeding with human islets was shown to function significantly better than free islets.(153, 154) EMPs have also been found to express high levels of key beta-cell specific genes and secrete quantities of insulin per cell similar to freshly isolated human islets in a glucose-regulated manner for more than three months *in vitro*.(153) Lung instead of pancreas-derived micro-scaffolds were chosen since most of the pancreatic matrix is derived from the exocrine organ (155) and the lung matrix may enable interaction between beta cells and endothelial cells.(156)

In this study, we sought to evaluate the function of the EMPs after implantation into hyperglycemic mice. We hypothesized that the EMPs would provide essential ECM macromolecules and structural support to maintain islet viability *in vivo*. We explored this approach with both mouse and human islets transplanted into immunodeficient mice.

4.2 Materials and Methods

4.2.1 Mouse Islet Isolation

All animals were housed under conventional conditions having free access to food and water. The care of the mice was in accordance with the guidelines approved by the Canadian Council on Animal Care. All experimental procedures were approved by the University of Alberta Research Ethics and Animal Use Committee (Study ID:

AUP00000419). Pancreatic islets were isolated from 8 to 12 week male BALB/c mice (Jackson Laboratories, CA). Before pancreatectomy, the common bile duct was cannulated and the pancreas was distended with 0.125 mg/mL cold Liberase TL Research Grade enzyme (Roche Diagnostics, Laval, QC, CA) in Hanks balanced salt solution (Sigma, St. Louis, MO, USA). Islets were isolated by digesting the pancreata at 37°C for 14 minutes with light shaking. Subsequent to the digestion phase, islets were purified from the pancreatic digests using histopaque-density gradients (1.108, 1.083 and 1.069 g/mL, Sigma, St. Louis, MO, USA). Islets were cultured in CMRL-1066 (Corning-cellgro, Manassas, VA, USA) supplemented with 10% fetal bovine serum, 1% L-glutamine (200 mM/L, Sigma, St. Louis, MO, USA), 1% sodium pyruvate (100 mM, Sigma, St. Louis, MO, USA), 1% non-essential amino acid 100x (Sigma, St. Louis, MO, USA), 100 U/mL penicillin-G and100 µg/mL streptomycin (Sigma Aldrich Canada Co., Oakville, ON, CA). A total of 5 mouse islet isolations were performed and all groups were randomized to receive islets from each isolation.

4.2.2 Human Islet Isolation

Human islets were isolated from a human pancreas procured from a multi-organ deceased donor transported to the clinical isolation center in cold preservation solution. The human islets were isolated implementing a modified Ricordi technique.(157, 158) All work was approved through the Health Research Ethics Board - Biomedical Panel of the University of Alberta. Written permission was obtained in all cases from the organ donor's family to use islets for experimental research. Processed human islets were only made available for research after failing to yield minimal mass required for clinical transplantation. Human

islets were cultured in clinical grade CMRL-1066 media (Media Tech, MT99-603-L) supplemented with insulin selenium-transferrin and insulin-like growth factor-1 at 22 °C and were received 24 hours after isolation.

4.2.3 Preparation of Decellularized Microscaffolds

Both cadaveric human and porcine lung derived 3D microscaffolds were engineered and prepared according to previously established protocols.(153, 154) Human and porcine lung tissue were stored at -80°C until required. The frozen tissue was cut into 5 – 8 mm diameter cylinders with a core drill press. Cores were sectioned into small slices, approximately 300 μm in thickness and decellularized into microscaffolds according to previously described methods.(153) Briefly, microscaffolds were washed twice in 1M NaCL for 30 minutes each, followed by 0.5 % Triton X-100 (Sigma Aldrich, St. Louis USA) for 1 minute x3. The micorscaffolds were then washed with distilled water twice for 60 minutes. Microscaffolds were then stored at 4°C overnight in PBS supplemented with 1000 U/mL penicillin-G, 1 mg/ml streptomycin (Sigma Aldrich, St. Louis USA). The pore size was not determined in this experiment. Mouse islets were seeded on porcine decellularized lung tissue, while human islets were seeded on human decellularized lung tissue derived from discarded surgical resection or cadaveric-derived lungs that could not be used for clinical transplantation. Permission for use of human cadaveric lung tissue was obtained through the Human Health Research Ethics Board – Biomedical Panel of the University of Alberta (Study ID: Pro00041552). Written permission was obtained in all cases from the organ donor's family to use the lung for experimental research. The lung was made available for research only after it was deemed unsuitable for clinical transplantation.

4.2.4 Seeding of Islets onto Microscaffolds

Prior to seeding, decellularized microscaffolds were washed three times with PBS to remove excess antibiotics then cultured in medium described above at 37°C, 5% CO_2 and saturated humidity for a minimum of 2 hours. For the pilot study, islets were seeded manually by pipetting the required islet dose directly onto the scaffold in minimal culture medium. For the remainder of the study, islets were aliquoted and re-suspended in low volume (3 ml) culture medium. The aliquoted islets and microscaffolds were transferred to a 500 cc glass pyrex bottle targeting 50 islets per micro-scaffold. The bottle was rotated at 5 rotations/minute on a roller-mixer (SRT9D, Stuart) at 37°C, 5% CO_2 and saturated humidity for 90 minutes. The seeded microscaffolds are referred to as endocrine micro-pancreata (EMPs).

4.2.5 Transplantation with Mouse Islets

Diabetes was chemically induced with streptozotocin (175 mg/kg i.p.) (Sigma, St. Louis, MO, USA) in adult immunodeficient C57BL/6 $RAG^{-/-}$ mice (Jackson Laboratories, Bar Harbor, ME, USA) at 12-14 weeks of age. Animals were considered diabetic after two consecutive non-fasting blood glucose measurements >15 mmol/L.

All transplant recipients received 500 islets ± 10% with a purity of 90% and were divided into three groups: a positive control group (n=9) with islet transplantation under the kidney capsule (KC500), a control group (n=8) with free islet transplantation into the intraperitoneal (IP500) cavity on the liver and stomach surfaces and a study group (n=9) with EMP implantation into the peritoneal cavity (EMP500). A fraction of the EMPs (10%) were removed from the study, stained with dithizone and enumerated to

extrapolate the number of EMPs per transplant (3 mg/ml dithizone, Sigma Aldrich Canada Co., Oakville, ON, CA).

4.2.6 Transplantation with Human Islets

A pilot study was initially conducted at the Hebrew University of Jerusalem to explore the potential impact of EMPs on islet function *in vivo.* 12 NOD-SCID mice (Charles River, Hollister, CA, USA) were implanted with EMPs subcutaneously at three doses: 150 islet equivalents (IEQ) ± 10 %, 200 IEQ ± 10 %, 500 IEQ ± 10 % and control empty scaffolds (n=3 per group). Human islets were manually seeded onto the EMPs for the pilot study. The second cohort of experiments was conducted at the University of Alberta using adult immunodeficient C57BL/6 $RAG^{-/-}$ mice (Jackson Laboratories, Bar Harbor, ME, USA). Diabetes was chemically induced with streptozotocin (175 mg/kg i.p.) (Sigma, St. Louis, MO, USA) for all mice and animals were considered diabetic after two consecutive non-fasting blood glucose measurements >15 mmol/L. Mice were separated into 3 groups: low dose Group A received EMPs seeded with a marginal therapeutic dose of 250 IEQ ± 10% (n=4), intermediate dose Group B received EMPs seeded with 500 IEQ ± 10% (n=4) and high dose Group C received EMPs seeded with 1000 IEQ ± 10% (n=4). Outcomes were compared with concurrent and recent historic controls from our laboratory of similar strain mice receiving 1000 IEQ ± 10% (n= 17) human islets transplanted beneath the renal capsule. All EMPs were implanted within the peritoneal cavity on the liver surface.

4.2.7 Assessment of Graft Function

After transplantation, non-fasting blood glucose levels were monitored three times per week (between 13:00 and 17:00) using a portable glucometer (OneTouch Ultra 2, LifeScan, CA, USA). Mice were considered normoglycemic at blood glucose levels maintained at <11.1 mmol/L throughout the study period. Intraperitoneal glucose tolerance tests (IPGTTs) were performed 6 weeks post-transplant to assess the capacity of the graft to respond to a glucose bolus. After 8 hours of fasting, mice were injected with 3 g/kg 25% dextrose intraperitoneally. Blood glucose levels were monitored at 0, 15, 30, 60 and 120 minutes post-dextrose infusion. A recovery nephrectomy was performed on all mice that received transplantation under the kidney capsule to confirm graft-dependent function. For mice transplanted with human islets, blood samples were obtained by cardiac puncture at the time of euthanasia (90 days post-transplantation) and human c-peptide levels were measured by ELISA (Ultrasensitive, Mercodia, Uppsala, Sweden). Normoglycemic mice received 3 g/kg 25% dextrose 15 minutes prior to collection.

4.2.8 Relative Quantitative Real-Time Polymerase Chain Reaction

RT-PCR was performed as previously described by *Sionov et al* (153). RNA was isolated by TriReagent (Sigma, St. Louis, MO, USA) then converted to cDNA using AB high capacity kit (Applied Biosystems). High precision TaqMan primers and TaqMan Gene Expression Master Mix in an ABI PRISM 7900HT Sequence Detection System (Applied Biosystems) were used (Table 1). Since no significant differences were observed between

the three different housekeeping genes, TATA-box binding protein (TBP), GAPDH and HPRT used as internal standards, TBP was used.

The threshold Cycle (Ct) of each gene for a given EMP sample was subtracted from the Ct of TBP of the same sample (Δ Ct), which was then subtracted from the Δ Ct of the donor islet sample ($\Delta\ \Delta$ Ct). The fold change in gene expression was calculated by the power of 2 of the $-\Delta\ \Delta$ Ct value ($2^{-\Delta\ \Delta Ct}$). Thus, the presence of other cell types within the EMP leads to a reduction in the insulin/TBP ratio.

Table 1. Reference sequences of TaqMan probes obtained from the Applied Biosystems TaqMan expression system.

Gene	Accession number	ABI primer RefSeq
TBP	**NM_003194.4**	**Hs99999910_m1**
GAPDH	**NM_002046.4**	**Hs99999905_m1**
HPRT-1	**NM_000194.2**	**Hs02800695_m1**
Insulin	**NM_000207.2**	**Hs02741908_m1**
Pdx-1	**NM_000209.3**	**Hs00236830_m1**

4.2.9 Histological Analysis

At 60 days post-transplantation, EMPs containing mouse islet grafts were explanted, fixed in formalin and subsequently embedded in paraffin. 5 μm sections were prepared and stained with Masson's trichrome to visualize connective tissue. Immunofluorescent double staining was performed using primary antibody of guinea pig anti-pig insulin (1:100; Dako, Carpinteria, CA, USA) and rabbit anti- CD31 (1:50; abcam, Cambridge, MA, USA) overnight at 4°C. Secondary antibody of goat anti-guinea pig (1:200; Rhodamine, Jackson ImmunoResearch Laboratories) and goat anti-rabbit (1:200; Fluorescein, Vector Laboratories, Burlingame, CA, USA) were used on the second day of staining. Samples were counterstained with DAPI in anti-fade mounting medium (ProLong, LifeTechnologies, Eugene, OR, USA). Slides were examined under fluorescent microscopy. Images were photographed using the appropriate filter with AxioVision imaging software. For EMPs seeded with human islets, grafts were explanted 90 days post-transplantation and processed as mentioned above. In addition to insulin staining, the grafts were double stained with rabbit anti-glucagon (1:200; abcam, MA, USA) for 2 h at 4°C. Secondary antibody consisting of goat anti-guinea pig (1:200 Rhodamine, Jackson) and goat anti-rabbit (1:200; Fluorescein, Vector Laboratories, Burlingame, CA, USA)

4.2.10 Statistical Analysis

Data are represented as means ± standard error of the mean (SEM). Area under the curve (AUC) for IPGTTs and differences between groups were calculated using student's t test. One-way ANOVA and Tukey's post-hoc test was used to compare human c-peptide levels. Kaplan-Meier survival function curves were compared using the log-rank

statistical method. Statistical analyses were performed using GraphPad Prism (GraphPad Software, La Jolla, CA, USA). A p value < 0.05 was considered significant.

4.3 Results

4.3.1 Subcutaneous Implantation of EMPs Reversed Hyperglycemia in NOD-SCID Mice

A pilot study was conducted at the Hebrew University of Jerusalem by Dr. Eduardo Mitrani group to investigate the potential benefits of the EMPs on *in vivo* islet function. Dithizone staining of the EMPs confirmed the presence of islets (Fig 4-1A). Mice receiving 150 IEQ were followed for 19 days post-transplant, primarily to evaluate the incorporation of EMPs into the host and the function of this novel approach. None of the animals in this group achieved normoglycemia, and were subsequently euthanatized to retrieve the EMPs. On macroscopic examination, the EMPs became vascularized and exhibited no signs of overt inflammation (data not shown). Real time PCR further confirmed the presence of islets, as evidenced by transcription of insulin and pancreatic and duodenal homeobox 1 (PDX-1) genes (Fig 4-1 B). Mice receiving 200 IEQ had reduced blood glucose levels in the first week of implantation (Fig 4-1 C). However, mice reverted to hyperglycemia by three weeks post-implant, most likely due to the small amount of transplanted islets. In contrast, mice receiving 500 IEQ were normoglycemic throughout the study period until the EMPs were retrieved 35 days post-transplantation (Fig 4-1C). In contrast, non-transplanted hyperglycemic control animal blood glucose levels increased rapidly leading to mortality within 5 to 8 days (Fig 4-1C). Dr. Eduardo Mitrani group completed this study at the Hebrew University of Jerusalem.

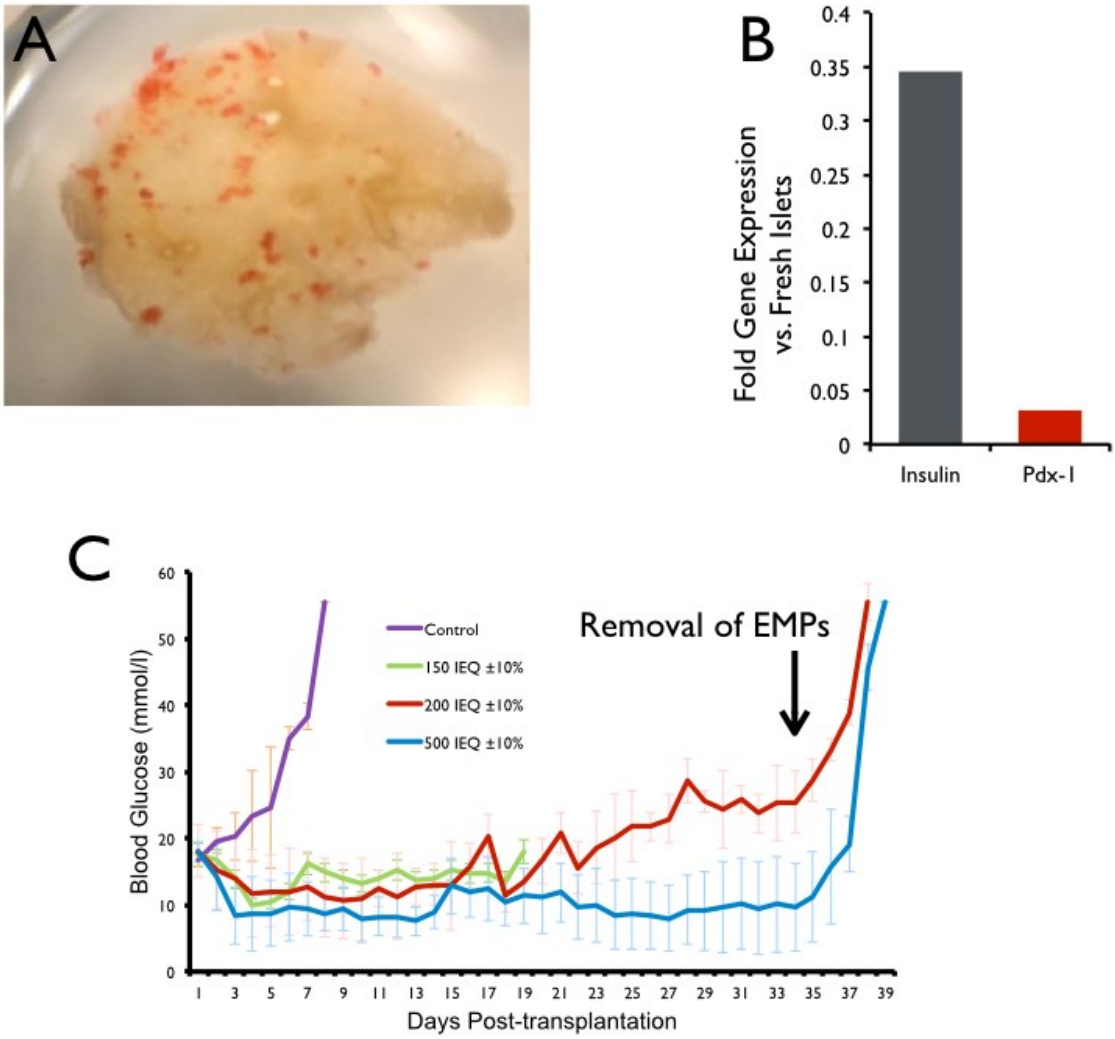

Fig 4-1. Pilot study of endocrine micro-pancreata (EMPs) implanted subcutaneously. (A) Dithizone stained EMP showing numerous human islets (red) seeded on the microscaffold. (B) Real time PCR gene expression of insulin and PDX-1 normalized to house-keeping gene TBP. Values are presented as fold expression per cell compared the values obtained from fresh islets (n=3, single analysis of pooled EMPs removed from three test animals). (C) Average non-fasting blood glucose levels for the three EMP doses implanted subcutaneously. Data are presented as mean ± SEM. This part of the study was completed at the Hebrew University of Jerusalem by our collaborators.

4.3.2 EMPs Improve Mouse Islet Graft Function After Intraperitoneal Transplantation

An immunodeficient mouse model was used in this study to investigate the impact of EMPs on islet neovascularization and engraftment, without confounding effects from either rejection or immunosuppressive agents. 66.7% of the mice transplanted with EMPs into the peritoneal cavity achieved normoglycemia (n=9) compared to only 12.5% (n=8) of the mice receiving free islets IP (p=0.018) (Fig 4-2 A). All 9 mice receiving murine islets under the kidney capsule became euglycemic. All mice were maintained until 60 days post-transplantation. For islets transplanted under the kidney capsule, used as a positive control, all mice underwent recovery nephrectomies and reverted to hyperglycemia within 48 h (Fig 4-2 B). However, recovery graft retrieval was not technically feasible in the EMP cases due to liver capsular adherence.

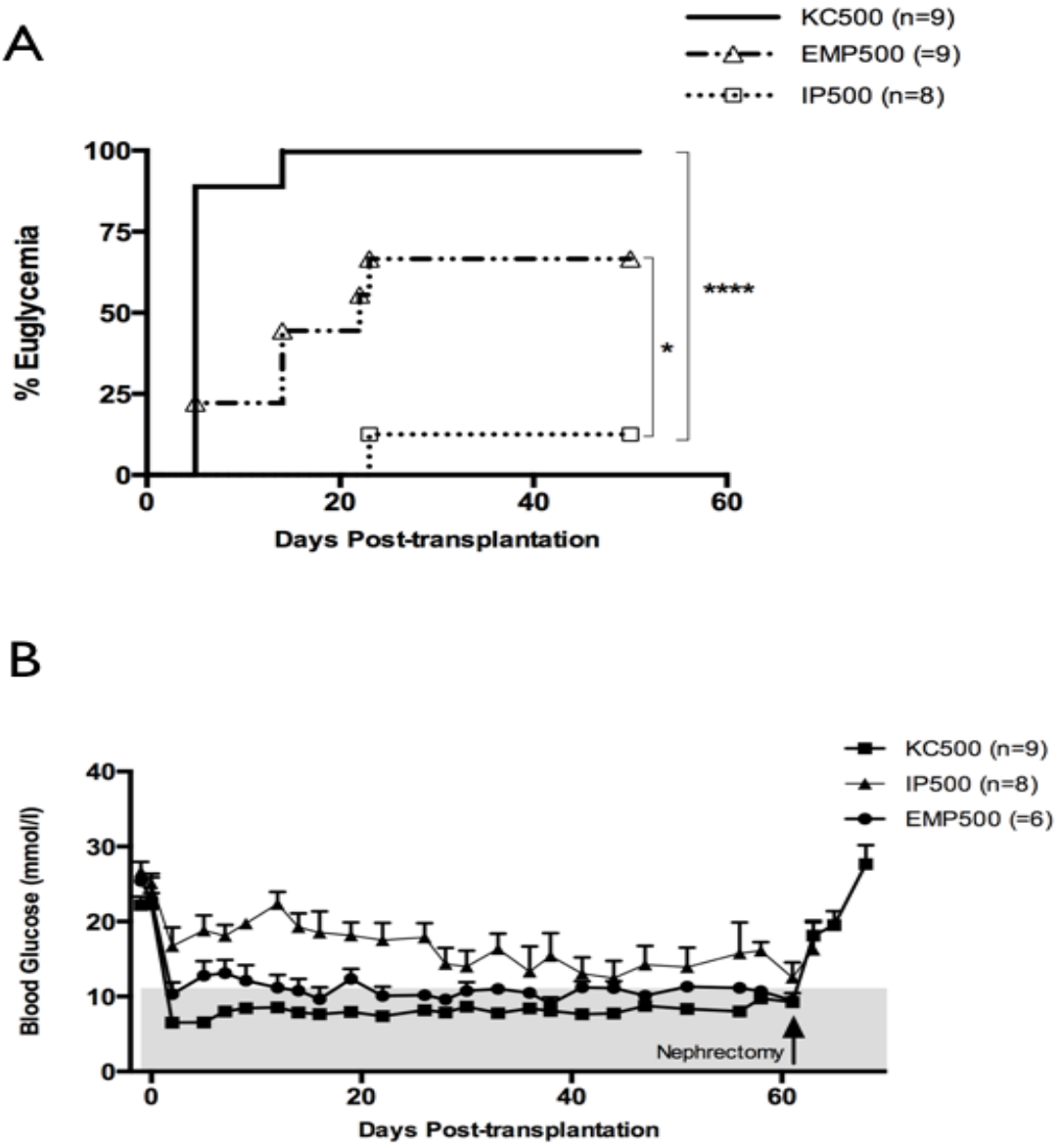

Fig 4-2. Long-term graft function after mouse islet transplantation. (A) The proportion of animals that achieved normoglycemia. Normoglycemia was restored in 6 animals from the EMP group compared to 1 from the IP group. This difference was statistically significant (P = 0.0183, Log-rank, Mantel-Cox test). All animals from the kidney capsule group were restored to normoglycemia compared to EMP and IP groups (P< 0.01 & 0.0001 respectively, Log-rank, Mantel-Cox test). Transplanted islets were from five different mouse isolations (n= 30 pancreata per isolation). (B) Average non-fasting blood glucose levels for kidney capsule group (KC500), intraperitoneal free islets group (IP500) and seeded microscaffold group (EMP500). Data are presented as mean ± SEM (one-sided error bars for clarity).

4.3.3 EMPs Improve Mouse Islet Graft Response to Glucose Challenge

Six weeks post-transplantation, mice underwent IPGTTs to evaluate graft function. IPGTTs were also performed on normoglycemic, age-matched, naïve mice as a control group (n=5). Blood glucose levels were lower in the EMP transplant group at all time points compared to the free IP islet group (Fig 3A). The area under the curve (AUC) for the EMP group was similar ($p > 0.05$, One way ANOVA with Tukey's post hoc test) to that of naïve mice but significantly lower ($p < 0.05$, One way ANOVA with Tukey's post hoc test) than the free IP islet transplant group (Fig 3B).

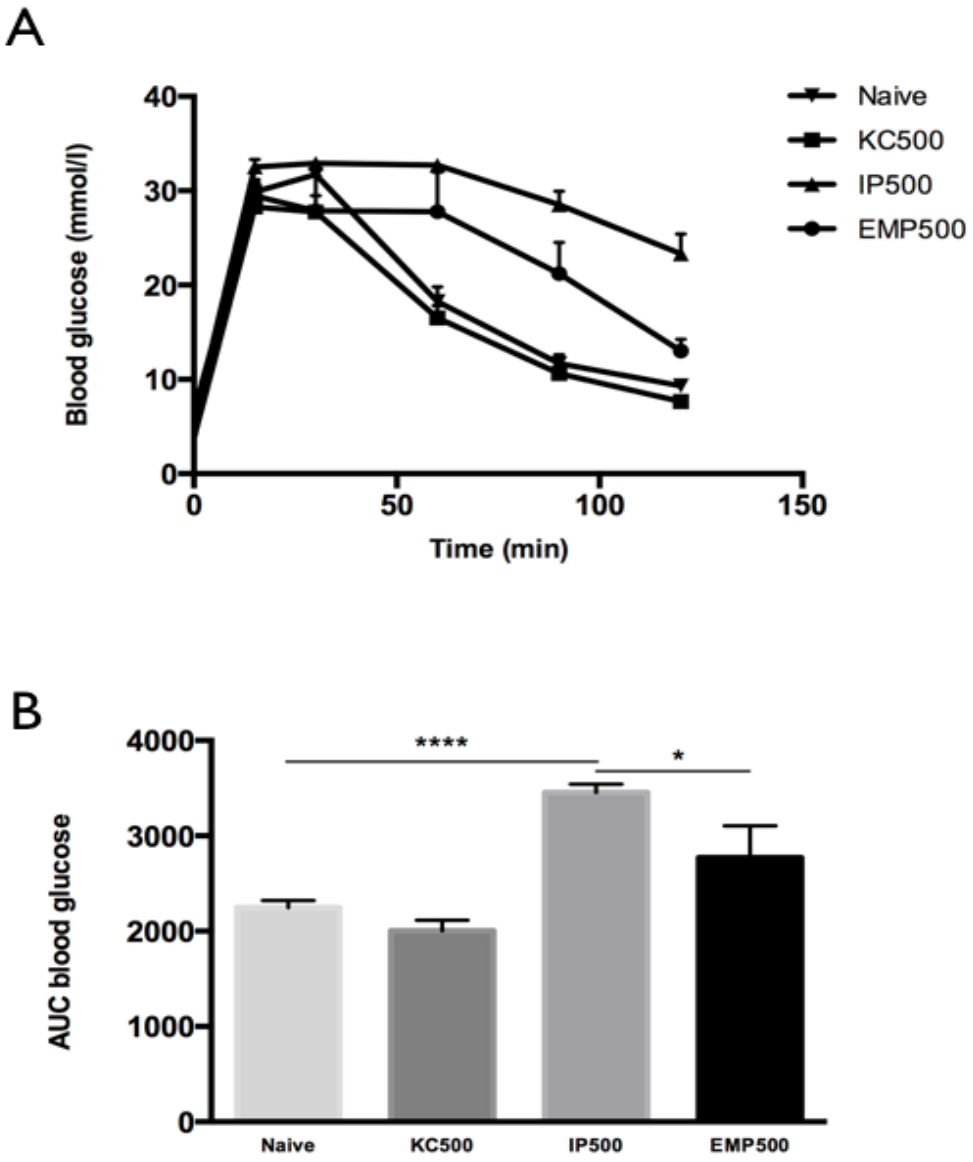

Fig 4-3. IPGTTs of the transplanted mouse islets six weeks post-transplantation. Blood glucose measurements after dextrose bolus (A) and AUC analysis (B) did not differ between Naïve (n=5) and EMP (n=6) groups ($p > 0.05$, One way ANOVA with Tukey's post hoc test). Animals that received free intraperitoneal islets (n=8) were intolerant to glucose challenge compared to EMP, Naïve and KC (n=9) groups (*$p < 0.05$, *** $p < 0.001$, and ****$p < 0.0001$ respectively; One way ANOVA with Tukey's post hoc test). All mice received 3 g/kg 25% dextrose i.p. bolus for this test and blood glucose measurements were taken at t = 0, 15, 30, 60, 90 and 120 min. Data are presented as mean ± SEM.

4.3.4 EMPs Support Islet Architecture

Islets seeded onto microscaffolds (EMPs) and subsequently transplanted exhibited normal morphology 60 days post-transplantation (Fig 4-4). An abundance of blood vessels were seen around the islets in the connective tissue-rich background (Figs 4-4 A and 4-4 C). Immunohistochemistry staining revealed a large number of insulin positive islets on the EMPs and stained positive for anti-CD31, which is primarily concentrated at the borders of endothelial cells (Figs 4-4 B and 4 D).

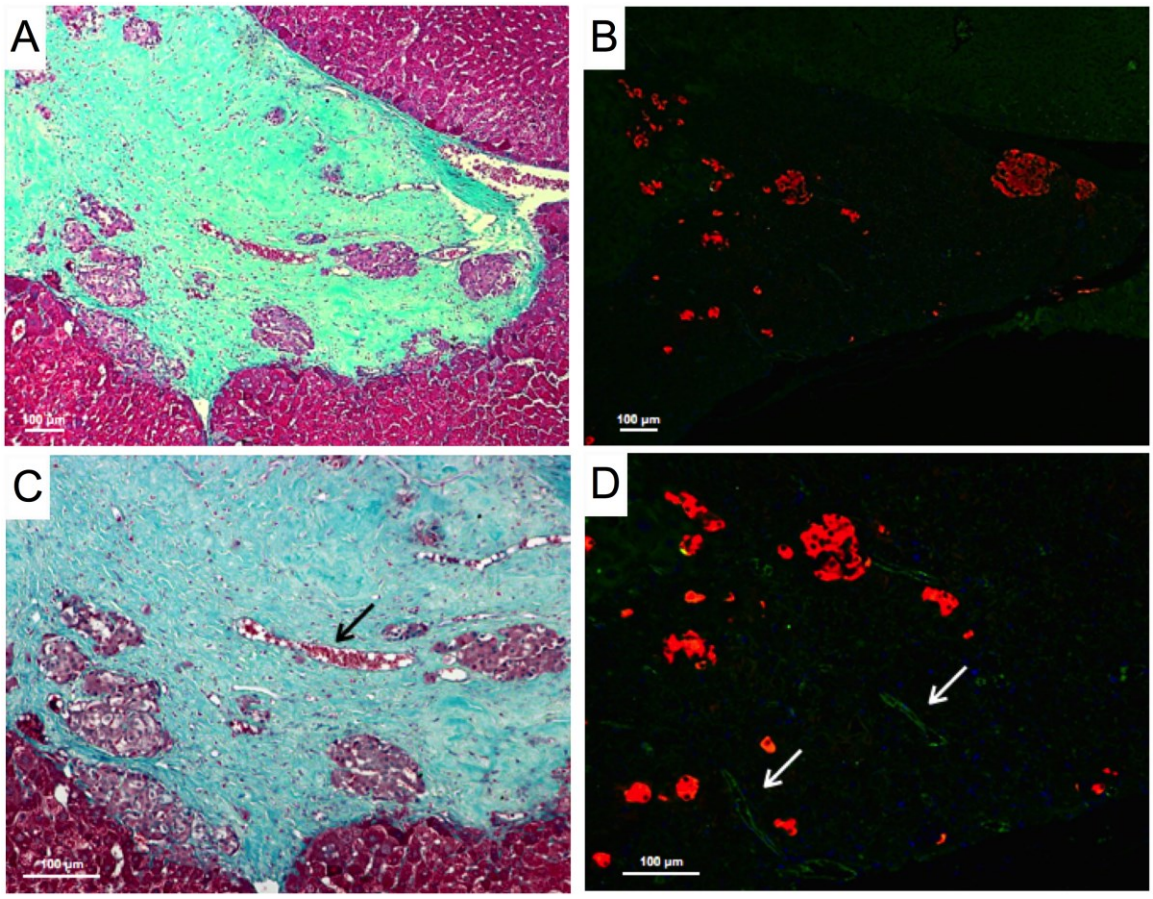

Fig 4-4. **Histological analysis of explanted islet grafts 60 days post-transplantation**. (A) Mason's trichrome staining of a cross-section of explanted EMP showing mouse islets of normal structure and size with surrounding background of collagen (blue), smooth muscles, erythrocytes (red) and scaffold-liver interface at (100x). (C) Mason's trichrome staining of mouse islets seeded on EMP at higher magnification (200x) showing erythrocyte filled blood vessel (arrow) with fluorescent staining of the same sections (B&D) to confirm the presence of insulin (red) and neovascularization (arrows) with positive anti-CD31 staining.

4.3.5 Micro-scaffolds Improve Human Islet Function After Intraperitoneal Transplantation

To further investigate impact of EMPs on intraperitoneal islet engraftment, we sought to determine EMP engraftment using human islets transplanted into immunodeficient mice. The human islet preparation had a purity of 69% and viability of 85%. Mice received low (250 IEQ), moderate (500 IEQ) or high (1000 IEQ) dose EMPs. Three mice receiving high dose EMPs (Group C) achieved normoglycemia (75%, n=4) as compared to 2 mice receiving moderate dose EMPs (Group B) (50%, n=4). All mice transplanted with low dose EMPs (Group A) failed to achieve normoglycemia throughout the study (0%, n=4). Compared to concurrent and recent historic renal subcapsular controls, 10 0f 17 mice (58.8%) achieved normoglycemia with transplantation of a marginal human islet dose of 1000 IEQ (Fig 4-5 A).

As expected, average non-fasting glucose levels were inversely proportional to transplanted islet dose (Fig 4-5 B). To confirm graft-dependent normoglycemia human c-peptide levels were measured in blood samples obtained by cardiac puncture at time of euthanasia 90 days post-transplantation. Seeding EMPs with higher islet mass resulted in higher stimulated human c-peptide levels (Fig 4-5 C). The average stimulated human c-peptide levels for group C was 1.23 ± 0.15 nmol/L compared to 0.39 ± 0.15 nmol/L and 0.08 ± 0.03 nmol/L for group B and A, respectively, confirming a dose-dependent response (Fig 4-5 C). This difference was statistically significant ($p<0.01$ and $p< 0.001$, respectively). The observed stimulated human c-peptide levels 90 days post-transplant corresponded to euglycemic function observed through daily non-fasting blood glucose levels (Fig 4-5 B).

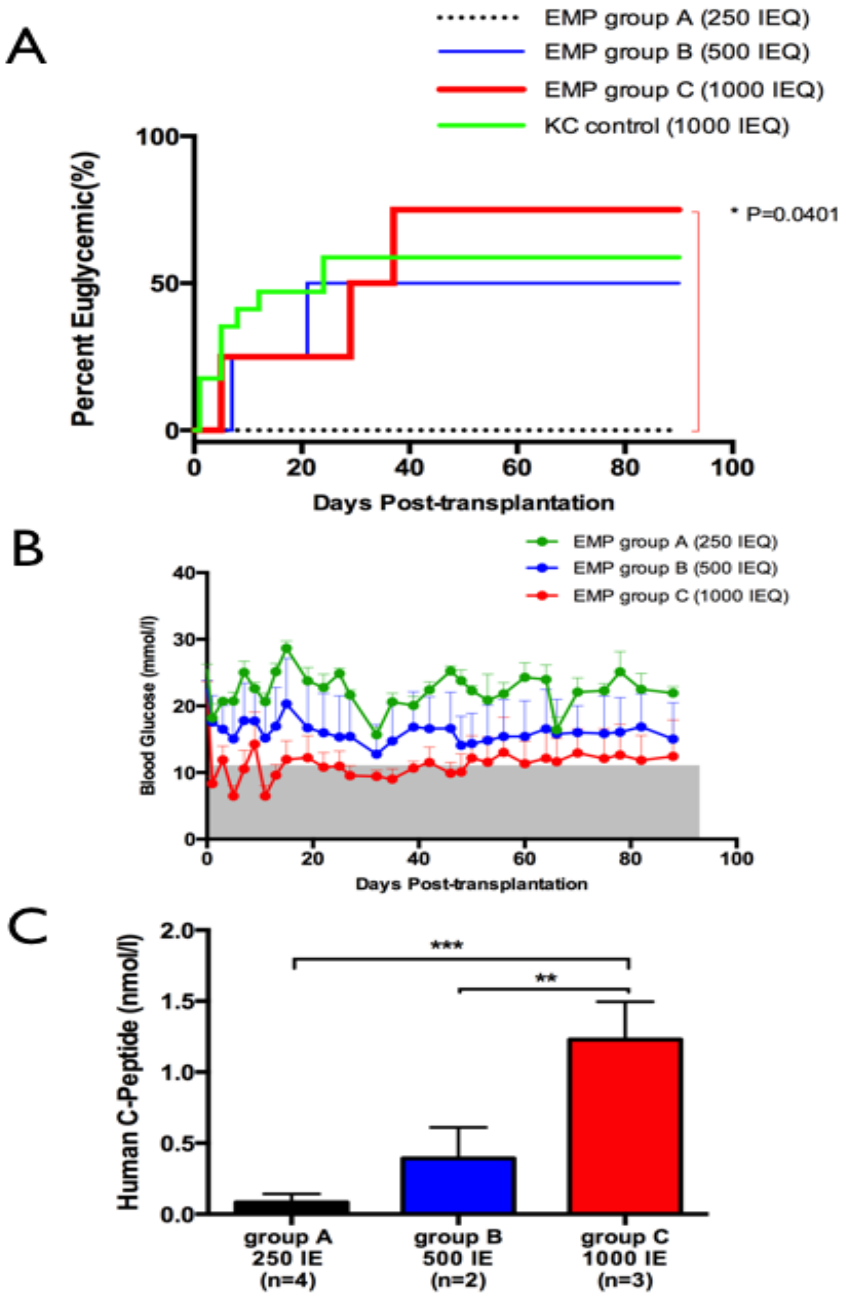

Fig 4-5. Long-term graft function after human islet transplantation. (A) The proportion of animals that achieved normoglycemia from the high dose EMP group C was significantly higher (p=0.0401) compared to the low dose EMP group A. However, this difference was not significant compared to the intermediate dose EMP group B and historical kidney capsule groups (p=0.671 and 0.889; respectively). (B) Average non-fasting blood glucose levels for all the groups were inversely proportional to transplanted islet dose. (C) Average stimulated human C-peptide levels for Group C was significantly higher than Groups A and B ($p<0.001$ and $p<0.01$, respectively; one way ANOVA with Tukey's multiple comparison test).

4.3.6 EMPs Maintained Insulin/Glucagon Positive Islets 90 Days Post-Transplantation

Immunohistochemistry staining was performed 90 days post-transplantation to evaluate islet insulin and glucagon content. Human islets maintained normal morphology and size with numerous blood vessels infiltrating the microscaffold (Fig 4-6 A). Islets stained positive for insulin and glucagon (Fig 4-6 B), which supports the observation of normal graft function and restoration of normoglycemia.

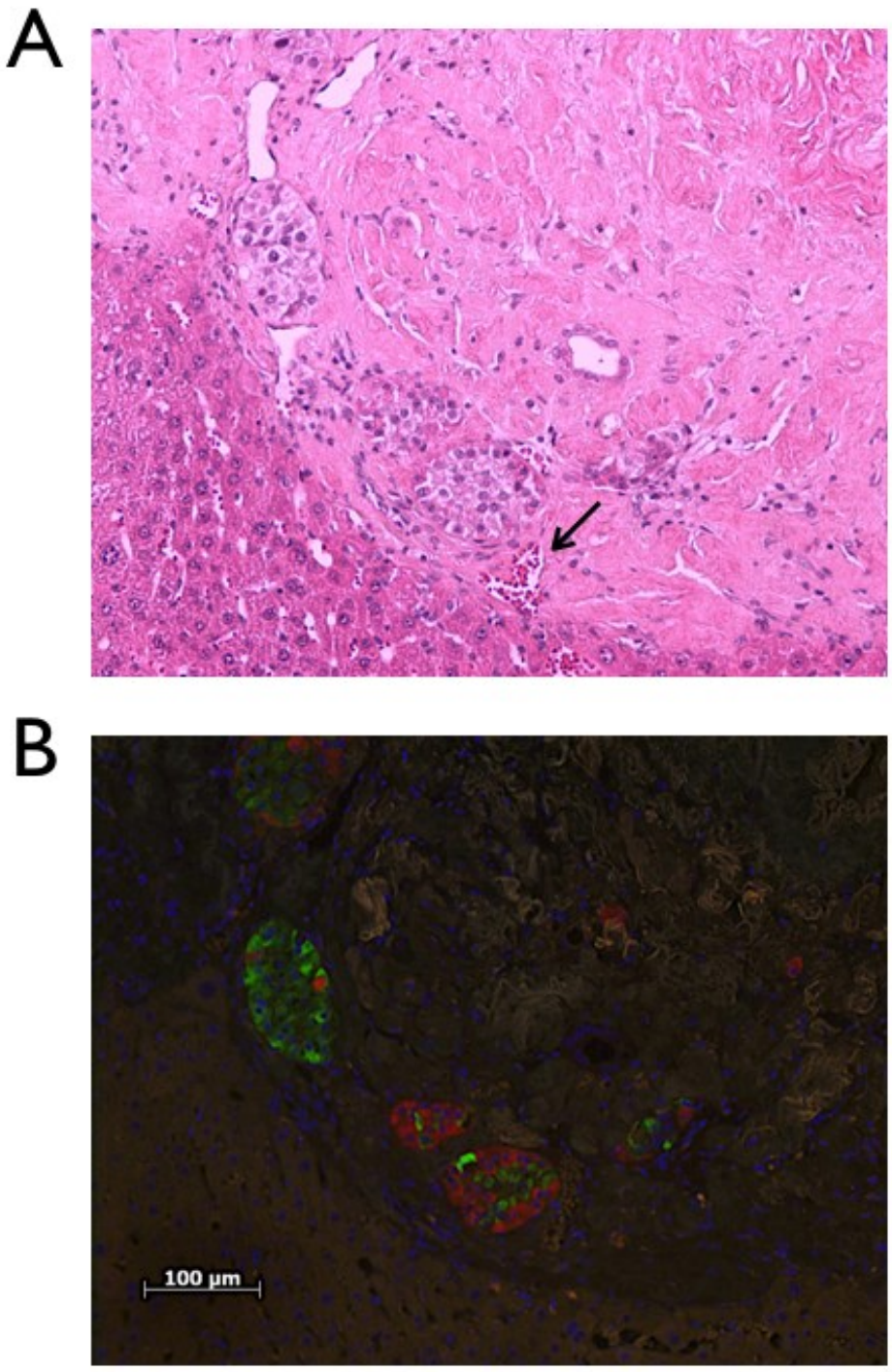

Fig 4-6. **Histological analysis of explanted islet grafts 90 days post-transplantation**. Hematoxylin and eosin staining of a cross-section of an explanted EMP graft on the surface of the liver showing multiple islets with an erythrocyte filled blood vessels (arrow). (B) Immunohistochemistry staining of the same section confirming the presence of insulin (red) and glucagon (green).

4.4 Discussion

In the present study, we explored the utility of a 3D lung-derived microscaffold to support islet engraftment in an alternative transplantation site. We postulated that the 3D microscaffolds provide ECM components of the islet microenvironment thereby generating favorable conditions to support islet functional survival *in vivo*.[33] EMPs have been shown to secrete insulin in a glucose-regulated manner for long periods in culture, in quantities comparable to freshly isolated islets.[32] In previous reports, supplementing islets with ECM components in culture resulted in superior islet function including collagen-IV, fibronectin,[25, 38] laminin,[24, 38] and others.[22, 23] Consistent with these results, our pilot study demonstrated potential for this approach where diabetes reversal was achieved with an islet mass as low as 500 IEQ in NOD-SCID mice with early evidence of neovascularization. Restoring the ECM microenvironment appears to reduce physiological stress experienced during and after islet isolation and consequently reducing non-immune-mediated cell death.

Cell death is one of the contributing factors of the initial islet mass loss. Anoikis, a form of apoptosis induced by disruption of cell-ECM interaction which is mediated by integrins may play an important role in islet graft loss.[39-41] Loss of peri-insular basement membrane following islet isolation has also been reportedly associated with apoptosis.[17-19] A study conducted by Pinkse *et al.* demonstrated that islets cultured on collagen-IV, laminin or fibronectin had significantly higher *in vitro* survival rates compared to collagen-I after 24 hours.[19] Blocking adhesion of β1 integrin subunit to its ECM significantly increased the number of dexoynucleotidyl transferase dUTP nick end labeling (TUNEL) positive cells in a further study.[42] The protective effect of ECM

molecules could therefore offer a window for islet graft vascularization and subsequent improvement of graft survival and function.

ECM components could additionally promote infiltration of host cells into the scaffold and the interaction between ECM proteins with cell surface integrins. Leukocyte and endothelial cell infiltration facilitated neovascularization in synthetic PLGA scaffolds.[43] Salvay *et al*. demonstrated that PLGA scaffolds significantly enhanced intra-islet microvascular density.[31] This finding further suggests that ECM proteins could play a key role in islet neovascularization. Consistent with these results, we observed an abundance of blood vessels infiltrating the EMPs around the islets in a connective tissue-rich background, which likely contributed to the beneficial effect observed in islet graft function. While in previous approaches, an individual ECM component is added to synthetic scaffolds, we utilized a natural source for the EMPs, rich in ECM components capable of preserving the spatial 3D relationship in an effort to provide a near natural microenvironment.[32, 33] We utilized lung tissue as a source to produce the microscaffolds rather than pancreas because of its large surface area lined by a basement membrane. In addition to providing the 3D scaffolding that supports the architecture and cell organization found in the native environment, the resulting microscaffolds were approximately 300μm in thickness, which allowed for free diffusion of gases and nutrients, thus reducing hypoxia.[32, 33] We chose decellularized human lung microscaffolds for the human islet study component as a means to test this clinically accessible and potentially approvable source of microscaffolds for future human clinical application.

The peritoneal cavity is an alternative site for islet transplantation as it offers a larger potential space compared to the liver, while avoiding liver-associated complications such as portal thrombosis or bleeding.[44] It is a readily accessible extravascular site with adequate arterial supply, and may be accessed readily with minimally invasive surgical techniques. Furthermore, the peritoneal cavity, like the pancreas, has dominant venous drainage to the portal circulation and may thus offer potential for physiologic insulin release and hepatic first pass metabolism. We further recognize that the peritoneal cavity may have more clinical relevance as compared to the subcutaneous site. Transplantation of unmodified islets into the peritoneal cavity has consistently been associated with poor engraftment and markedly impaired function in multiple previous studies, and has not worked effectively for human islet engraftment in patients.[45-47] Consistent with these previous findings, we observed severely impaired islet function when unmodified islets were implanted intraperitoneally.

In the current study, we observed significantly enhanced functional engraftment with reversal of diabetes in both murine and human islets when transplanted intraperitoneally with EMPs. One of the limitations of using the intraperitoneal site is an inability to effectively recover implanted islet grafts due to their adherent nature post procedure.[48] Application of glucose-stimulated human-specific c-peptide assays in the present study allowed us to confirm that normoglycemia resulted from successful engraftment of human islets. Indeed, we observed substantial circulating stimulated human c-peptide levels quantifiably comparable to levels observed in our human subjects receiving intraportal islet infusions resulting in insulin-independence (1.23 ± 0.15 nmol/L in mice bearing intraperitoneal EMPs vs. 1.62 ± 0.07 nmol/L in human subjects receiving

islet transplants).[49] A dose-response relationship between non-fasting blood glucose levels and c-peptide levels was observed. The EMPs stained positive for insulin and glucagon 90 days post-transplantation, supporting the contribution of the islet graft to the achievement of normoglycemia. Furthermore, mice achieved normoglycemia with an islet mass as low as 500 IEQ. To our knowledge, this is the lowest intraperitoneal human islet mass that has resulted in normoglycemia in a mouse model. Of note that, rodents are resistant to human insulin and they require significantly higher doses of insulin to reverse hyperglycemia.[50] This reduction in islet mass renews interest in the peritoneal cavity for islet transplantation and potentially for future application with stem cell-derived or xenogeneic cell transplant sources.

It has been documented that immunosuppressive agents are toxic for pancreatic islet function.[51] For instance, tacrolimus, which is one of the most effective drugs to prevent rejection, has been associated with a decrease in insulin gene expression and insulin secretion as well as graft revascularization.[51, 52] In a recent report, supplementing islets with synthetic antiaging glycopeptide was shown to be cytoprotective as it resulted in improvement of islet graft survival and insulin secretion.[52] One of the new immunosuppressive approaches is targeting the lymophocytic inotropic purinergic P2X receptor (P2X7R) that has been shown to play an important role in islet allograft rejection.[53] The use of P2X7R inhibitors delayed islet allograft rejection *in vivo,* and induced hyporesponsiveness toward donor antigens.[53] The use of anti-CD3, anti-thymoglobulin, CXCR1 and CXCR2 blockers are promising new approaches that were shown to be less toxic alternatives for the currently used immunosuppressive agents.[54-57] The use of CXCR4 antagonist mobilized autologous

hematopoietic stem cells and prolonged islet allograft survival in C57BL/6 mice.[58] For patients with T1DM, the presence of autoimmune response is another factor that could compromise the transplanted islet graft function.[54] In Vergani et al., the prolonged use of low dose murine anti-thymoglobulin (mATG) with CTLA4-Ig abrogated the autoimmune response, delayed allograft rejection and prolonged islet allograft survival in NOD mouse model.[59] This novel approach reversed diabetes in newly hyperglycemic NOD mice that maintained normoglycaemia for 60 days of follow up.[59] In the present study, we have used an immunocompromised mouse model to investigate the impact of EMPs on islet graft survival and function without cofounding effects from rejection and immunosuppressive agents. In future studies, it would be desirable to transplant EMPs into immunocompetent mouse model implementing novel immunosuppressive approaches to facilitate the transition to clinical transplantation.

In conclusion, we report reversal of diabetes in an immunodeficient mouse model using either subcutaneous or intraperitoneal EMP transplantation. In this approach, we modified the local islet microenvironment by providing a wide variety of ECM macromolecules to enhance graft survival and function. Sionov *et al*, has previously characterized the EMPs demonstrating significant morphological changes, while in culture, resulting in contraction and folding of the EMP, which ultimately becomes a small sphere varying from 0.7 to 1.5 mm in diameter.[32] Furthermore, this micro-organ was shown to contain endocrine components of the natural pancreas and capable of producing insulin in glucose-regulated manner consistent with our *in vivo* findings. Of especial importance is the ability of EMPs to promote vascularization, which is an essential trait for β-cells survival. Additionally, utilization of an alternative extravascular

site could potentially ameliorate IBMIR and provide an efficacious means of beta cell replacement when islet intra-portal infusion is contraindicated. This approach represents a significant improvement in bioengineered scaffolding and a transition from using synthetic biomaterials to more natural sources. This transplant technique is potentially clinically applicable and easily translatable using human-grade human-derived materials.

Chapter 5

General Discussion and Future Directions

5.1 Thesis Summary and Significance

The aim of this graduate work is to study existing mouse models for cellular transplantation and to critically examine their clinical application to diseases of the pancreas. The first part of this work focuses on animal research in the field of pancreatic cancer. It would be of value in pancreatic cancer management to have a reliable mouse model capable of predicting effective chemotherapy. We aim to establish a direct xenograft model in which a fresh biopsied tumor is implanted into immunodeficient mouse model. Analysis and drug testing on the specific tumor implanted are of a great value in predicting the appropriate chemotherapy for that particular cancer. Such a personalized approach would have the potential to improve the grave prognosis of pancreatic cancer. The content of this thesis evaluates a new methodology for cellular transplantation, utilizing a previously established Device-Less technology that proved to be superior to the unmodified subcutaneous space. In addition, it addresses a potential drug-drug interaction between gemcitabine and erlotinib, an FDA-approved treatment option for pancreatic cancer.(98) We are currently investigating the impact of this interaction in a mouse model using FLT PET tracer in a mouse model.

The second part of this thesis describes a novel methodology for pancreatic islet transplantation. In this approach, pancreatic islets are seeded onto organ-derived microscaffolds, which provide a wide variety of extracellular matrix macromolecules.

The microscaffolds are subsequently transplanted into the peritoneal cavity. Providing the essential extracellular matrix proteins restores the microenvironment of the pancreatic islet, which resulted into superior islet function and reduced the required transplanted islet mass in an extravascular site. If successfully translated to the clinic, this approach could be of a great clinical value since the peritoneal cavity is easily accessible and protect islet from direct contact with circulating immune cells.

5.2 Prevascularization of the Implantation Site and its Clinical Importance

We have shown earlier that utilizing the DL approach significantly accelerated cancer growth in a mouse model. However, we did not see a difference in engraftment rates, most likely a result of the cell lines adapting to growth in culture.(97) We recognize the 1 x 10^6 cells per implant used here is the standard cell mass implantation, which usually has a very high success rate in well-established cell lines.(59) Had we implanted fewer cells, we may have uncovered differences in engraftment efficiency between the SQ and DL sites. In future studies, it would be interesting to repeat the experiment with a marginal cell mass, such as 2 x 10^5, to compare the rate of engraftment as well as cancer growth rates.

We have also shown the feasibility of this approach in direct xenografts. Despite not being successful in our PDX study, we have seen a robust engraftment and growth in mouse-derived xengrafts. Of note, the sample size in our PDX study was not large enough to fairly evaluate this approach and two out the three samples used were from

suspected liver metastasis in which the presence of cancer cells was not confirmed. In future studies, it would be of value to increase the sample size to properly assess the use of this method. If successful, the DL approach would be of great significance in personalized medicine to facilitate PDX. Taking advantage of accelerated tumor growth, and potentially higher engraftment rates, personalized cancer grafts would be sooner available for drug testing.

5.3 Closing Remarks and Futures Studies

The content of this thesis describes two different approaches to improve cellular implantation in animal models. However, it is important to further explore the utility of these approaches to capitalize on the significantly improved outcomes in experimental animal models to eventually translate that to the clinic.

In future studies, it is planned to further pursue the DL technology in personalized medicine. We currently have the ethics committee approval to enroll more patients with gastrointestinal cancers in this study. Pancreatic caner biopsies, and possibly other gastrointestinal tumors, are planned to be implanted into NSG mice to properly assess the utility of this technique. Histological analysis of the resulting tumors and bioassay will be compared to the clinical data of the patients. When successful, that could open the path for personalized medicine where cancer treatment for an individual patient can be guided by the outcomes in the mouse model.

In an ongoing study, we are studying the interaction between tyrosine kinase inhibitors and nucleoside analogues and its impact on the treatment of pancreatic cancer. NSG mice

implanted with MIA-PaCa-2 cell line are being evaluated with [^{18}F]FLT PET scanner in the presence and absence of erlotinib and NBMPR-P. It is important to determine if a significant drug-drug interaction between gemcitabine and erlotinib exist since the combination is an approved treatment option for advanced pancreatic cancer.

References

1. Siegel R, Desantis C, Jemal A. Colorectal cancer statistics, 2014. CA Cancer J Clin. 2014;64(2):104-17.

2. Pancreatic cancer statistics. Canadian Cancer Society. Available at: http://www.cancer.ca/en/cancer-information/cancer-type/pancreatic/statistics/?region=sk. Accessed on Dec 8, 20132013.

3. Ryan DP, Hong TS, Bardeesy N. Pancreatic adenocarcinoma. N Engl J Med. 2014;371(22):2140-1.

4. Silverman DT. Risk factors for pancreatic cancer: a case-control study based on direct interviews. Teratog Carcinog Mutagen. 2001;21(1):7-25.

5. Regine WF, John WJ, Mohiuddin M. Current and emerging treatments for pancreatic cancer. Drugs Aging. 1997;11(4):285-95.

6. Lowenfels AB, Maisonneuve P. Risk factors for pancreatic cancer. J Cell Biochem. 2005;95(4):649-56.

7. Mak IW, Evaniew N, Ghert M. Lost in translation: animal models and clinical trials in cancer treatment. Am J Transl Res. 2014;6(2):114-8.

8. Johnson JI, Decker S, Zaharevitz D, Rubinstein LV, Venditti JM, Schepartz S, et al. Relationships between drug activity in NCI preclinical in vitro and in vivo models and early clinical trials. Br J Cancer. 2001;84(10):1424-31.

9. Kim MP, Evans DB, Wang H, Abbruzzese JL, Fleming JB, Gallick GE. Generation of orthotopic and heterotopic human pancreatic cancer xenografts in immunodeficient mice. Nat Protoc. 2009;4(11):1670-80.

10. Hidalgo M, Bruckheimer E, Rajeshkumar NV, Garrido-Laguna I, De Oliveira E, Rubio-Viqueira B, et al. A pilot clinical study of treatment guided by personalized tumorgrafts in patients with advanced cancer. Mol Cancer Ther. 2011;10(8):1311-6.

11. Beckhove P, Schütz F, Diel IJ, Solomayer EF, Bastert G, Foerster J, et al. Efficient engraftment of human primary breast cancer transplants in nonconditioned NOD/Scid mice. Int J Cancer. 2003;105(4):444-53.

12. Busnardo AC, DiDio LJ, Tidrick RT, Thomford NR. History of the pancreas. Am J Surg. 1983;146(5):539-50.

13. Fitzgerald PJ. Medical anecdotes concerning some diseases of the pancreas. Monogr Pathol. 1980;21:1-29.

14. Brunschwig A. The Surgical Treatment of Carcinoma of the Body of the Pancreas. Ann Surg. 1944;120(3):406-16.

15. Whipple AO. Pancreaticoduodenectomy for Islet Carcinoma : A Five-Year Follow-Up. Ann Surg. 1945;121(6):847-52.

16. Brady AC, Martino MM, Pedraza E, Sukert S, Pileggi A, Ricordi C, et al. Proangiogenic Hydrogels Within Macroporous Scaffolds Enhance Islet Engraftment in an Extrahepatic Site. Tissue Eng Part A. 2013.

17. Lowenfels AB, Maisonneuve P. Epidemiology and risk factors for pancreatic cancer. Best Pract Res Clin Gastroenterol. 2006;20(2):197-209.

18. Lin Y, Tamakoshi A, Kawamura T, Inaba Y, Kikuchi S, Motohashi Y, et al. A prospective cohort study of cigarette smoking and pancreatic cancer in Japan. Cancer Causes Control. 2002;13(3):249-54.

19. Ben Q, Xu M, Ning X, Liu J, Hong S, Huang W, et al. Diabetes mellitus and risk of pancreatic cancer: A meta-analysis of cohort studies. Eur J Cancer. 2011;47(13):1928-37.

20. Huxley R, Ansary-Moghaddam A, Berrington de González A, Barzi F, Woodward M. Type-II diabetes and pancreatic cancer: a meta-analysis of 36 studies. Br J Cancer. 2005;92(11):2076-83.

21. Chari ST, Leibson CL, Rabe KG, Ransom J, de Andrade M, Petersen GM. Probability of pancreatic cancer following diabetes: a population-based study. Gastroenterology. 2005;129(2):504-11.

22. Fisher WE, Boros LG, Schirmer WJ. Insulin promotes pancreatic cancer: evidence for endocrine influence on exocrine pancreatic tumors. The Journal of surgical research. 1996;63(1):310-3.

23. Li D, Yeung SC, Hassan MM, Konopleva M, Abbruzzese JL. Antidiabetic therapies affect risk of pancreatic cancer. Gastroenterology. 2009;137(2):482-8.

24. Decensi A, Puntoni M, Goodwin P, Cazzaniga M, Gennari A, Bonanni B, et al. Metformin and cancer risk in diabetic patients: a systematic review and meta-analysis. Cancer Prev Res (Phila). 2010;3(11):1451-61.

25. White PB, True EM, Ziegler KM, Wang SS, Swartz-Basile DA, Pitt HA, et al. Insulin, leptin, and tumoral adipocytes promote murine pancreatic cancer growth. J Gastrointest Surg. 2010;14(12):1888-94.

26. Jiao L, Berrington de Gonzalez A, Hartge P, Pfeiffer RM, Park Y, Freedman DM, et al. Body mass index, effect modifiers, and risk of pancreatic cancer: a pooled study of seven prospective cohorts. Cancer Causes Control. 2010;21(8):1305-14.

27. Li D, Morris JS, Liu J, Hassan MM, Day RS, Bondy ML, et al. Body mass index and risk, age of onset, and survival in patients with pancreatic cancer. JAMA. 2009;301(24):2553-62.

28. Silverman DT, Swanson CA, Gridley G, Wacholder S, Greenberg RS, Brown LM, et al. Dietary and nutritional factors and pancreatic cancer: a case-control study based on direct interviews. J Natl Cancer Inst. 1998;90(22):1710-9.

29. Z'graggen K, Warshaw AL, Werner J, Graeme-Cook F, Jimenez RE, Fernández-Del Castillo C. Promoting effect of a high-fat/high-protein diet in DMBA-induced ductal pancreatic cancer in rats. Ann Surg. 2001;233(5):688-95.

30. Lin Y, Kikuchi S, Tamakoshi A, Yagyu K, Obata Y, Inaba Y, et al. Dietary habits and pancreatic cancer risk in a cohort of middle-aged and elderly Japanese. Nutr Cancer. 2006;56(1):40-9.

31. Herrington MK, Permert J, Kazakoff KR, Pour PM, Zuker KA, Bilchik AJ, et al. Effects of high fat diet and cholecystokinin receptor blockade on pancreatic growth and tumor initiation in the hamster. Carcinogenesis. 1993;14(5):1021-6.

32. Bartsch DK, Gress TM, Langer P. Familial pancreatic cancer--current knowledge. Nat Rev Gastroenterol Hepatol. 2012;9(8):445-53.

33. Shi C, Hruban RH, Klein AP. Familial pancreatic cancer. Arch Pathol Lab Med. 2009;133(3):365-74.

34. Krejs GJ. Pancreatic cancer: epidemiology and risk factors. Dig Dis. 2010;28(2):355-8.

35. Duell EJ, Lucenteforte E, Olson SH, Bracci PM, Li D, Risch HA, et al. Pancreatitis and pancreatic cancer risk: a pooled analysis in the International Pancreatic Cancer Case-Control Consortium (PanC4). Ann Oncol. 2012;23(11):2964-70.

36. Raimondi S, Lowenfels AB, Morselli-Labate AM, Maisonneuve P, Pezzilli R. Pancreatic cancer in chronic pancreatitis; aetiology, incidence, and early detection. Best Pract Res Clin Gastroenterol. 2010;24(3):349-58.

37. Jiao L, Silverman DT, Schairer C, Thiébaut AC, Hollenbeck AR, Leitzmann MF, et al. Alcohol use and risk of pancreatic cancer: the NIH-AARP Diet and Health Study. Am J Epidemiol. 2009;169(9):1043-51.

38. Gapstur SM, Jacobs EJ, Deka A, McCullough ML, Patel AV, Thun MJ. Association of alcohol intake with pancreatic cancer mortality in never smokers. Arch Intern Med. 2011;171(5):444-51.

39. Holst JJ. The physiology of glucagon-like peptide 1. Physiol Rev. 2007;87(4):1409-39.

40. Matveyenko AV, Dry S, Cox HI, Moshtaghian A, Gurlo T, Galasso R, et al. Beneficial endocrine but adverse exocrine effects of sitagliptin in the human islet amyloid polypeptide transgenic rat model of type 2 diabetes: interactions with metformin. Diabetes. 2009;58(7):1604-15.

41. Nachnani JS, Bulchandani DG, Nookala A, Herndon B, Molteni A, Pandya P, et al. Biochemical and histological effects of exendin-4 (exenatide) on the rat pancreas. Diabetologia. 2010;53(1):153-9.

42. Elashoff M, Matveyenko AV, Gier B, Elashoff R, Butler PC. Pancreatitis, pancreatic, and thyroid cancer with glucagon-like peptide-1-based therapies. Gastroenterology. 2011;141(1):150-6.

43. Cure P, Pileggi A, Alejandro R. Exenatide and rare adverse events. N Engl J Med. 2008;358(18):1969-70; discussion 71-2.

44. Ojajärvi A, Partanen T, Ahlbom A, Boffetta P, Hakulinen T, Jourenkova N, et al. Risk of pancreatic cancer in workers exposed to chlorinated hydrocarbon solvents and related compounds: a meta-analysis. Am J Epidemiol. 2001;153(9):841-50.

45. Andreotti G, Silverman DT. Occupational risk factors and pancreatic cancer: a review of recent findings. Mol Carcinog. 2012;51(1):98-108.

46. Ulrich AB, Schmied BM, Standop J, Schneider MB, Pour PM. Pancreatic cell lines: a review. Pancreas. 2002;24(2):111-20.

47. Lee JJ, Huang J, England CG, McNally LR, Frieboes HB. Predictive modeling of in vivo response to gemcitabine in pancreatic cancer. PLoS Comput Biol. 2013;9(9):e1003231.

48. Pour P, Krüger FW, Althoff J, Cardesa A, Mohr U. Cancer of the pancreas induced in the Syrian golden hamster. Am J Pathol. 1974;76(2):349-58.

49. Chester JF, Gaissert HA, Ross JS, Malt RA. Pancreatic cancer in the Syrian hamster induced by N-nitrosobis(2-oxopropyl)-amine: cocarcinogenic effect of epidermal growth factor. Cancer Res. 1986;46(6):2954-7.

50. Fujii H, Egami H, Chaney W, Pour P, Pelling J. Pancreatic ductal adenocarcinomas induced in Syrian hamsters by N-nitrosobis(2-oxopropyl)amine contain a c-Ki-ras oncogene with a point-mutated codon 12. Mol Carcinog. 1990;3(5):296-301.

51. Dissin J, Mills LR, Mains DL, Black O, Webster PD. Experimental induction of pancreatic adenocarcinoma in rats. J Natl Cancer Inst. 1975;55(4):857-64.

52. Wei D, Xiong HQ, Abbruzzese JL, Xie K. Experimental animal models of pancreatic carcinogenesis and metastasis. Int J Gastrointest Cancer. 2003;33(1):43-60.

53. Osvaldt AB, Wendt LR, Bersch VP, Backes AN, de Cássia A Schumacher R, Edelweiss MI, et al. Pancreatic intraepithelial neoplasia and ductal adenocarcinoma induced by DMBA in mice. Surgery. 2006;140(5):803-9.

54. Roebuck BD, Longnecker DS. Species and rat strain variation in pancreatic nodule induction by azaserine. J Natl Cancer Inst. 1977;59(4):1273-7.

55. Kern SE. Molecular genetic alterations in ductal pancreatic adenocarcinomas. Med Clin North Am. 2000;84(3):691-5, xi.

56. Rangarajan A, Weinberg RA. Opinion: Comparative biology of mouse versus human cells: modelling human cancer in mice. Nat Rev Cancer. 2003;3(12):952-9.

57. Morioka CY, Saito S, Ohzawa K, Watanabe A. Homologous orthotopic implantation models of pancreatic ductal cancer in Syrian golden hamsters: which is better for metastasis research--cell implantation or tissue implantation? Pancreas. 2000;20(2):152-7.

58. Abraham AT, Shah SR, Davidson BR. The HaP-T1 Syrian golden hamster pancreatic cancer model: cell implantation is better than tissue implantation. Pancreas. 2004;29(4):320-3.

59. Marincola FM, Drucker BJ, Siao DY, Hough KL, Holder WD. The nude mouse as a model for the study of human pancreatic cancer. The Journal of surgical research. 1989;47(6):520-9.

60. Mohammad RM, Al-Katib A, Pettit GR, Vaitkevicius VK, Joshi U, Adsay V, et al. An orthotopic model of human pancreatic cancer in severe combined immunodeficient mice: potential application for preclinical studies. Clin Cancer Res. 1998;4(4):887-94.

61. Alves F, Contag S, Missbach M, Kaspareit J, Nebendahl K, Borchers U, et al. An orthotopic model of ductal adenocarcinoma of the pancreas in severe combined immunodeficient mice representing all steps of the metastatic cascade. Pancreas. 2001;23(3):227-35.

62. Alves F, Borchers U, Padge B, Augustin H, Nebendahl K, Klöppel G, et al. Inhibitory effect of a matrix metalloproteinase inhibitor on growth and spread of human pancreatic ductal adenocarcinoma evaluated in an orthotopic severe combined immunodeficient (SCID) mouse model. Cancer Lett. 2001;165(2):161-70.

63. Trevino JG, Summy JM, Lesslie DP, Parikh NU, Hong DS, Lee FY, et al. Inhibition of SRC expression and activity inhibits tumor progression and metastasis of human pancreatic adenocarcinoma cells in an orthotopic nude mouse model. Am J Pathol. 2006;168(3):962-72.

64. Killion JJ, Radinsky R, Fidler IJ. Orthotopic models are necessary to predict therapy of transplantable tumors in mice. Cancer Metastasis Rev. 1998;17(3):279-84.

65. Celli JP. Stromal interactions as regulators of tumor growth and therapeutic response: A potential target for photodynamic therapy? Isr J Chem. 2012;52(8-9):757-66.

66. Peterson JK, Houghton PJ. Integrating pharmacology and in vivo cancer models in preclinical and clinical drug development. Eur J Cancer. 2004;40(6):837-44.

67. Houghton PJ, Morton CL, Tucker C, Payne D, Favours E, Cole C, et al. The pediatric preclinical testing program: description of models and early testing results. Pediatr Blood Cancer. 2007;49(7):928-40.

68. Nicolson GL. Cancer metastasis: tumor cell and host organ properties important in metastasis to specific secondary sites. Biochim Biophys Acta. 1988;948(2):175-224.

69. Jimeno A, Feldmann G, Suárez-Gauthier A, Rasheed Z, Solomon A, Zou GM, et al. A direct pancreatic cancer xenograft model as a platform for cancer stem cell therapeutic development. Mol Cancer Ther. 2009;8(2):310-4.

70. Morioka CY, Saito S, Machado MC, Jukemura J, Bacchella T, Watanabe A. Different pattern of metastasis in liver implanted pancreatic cancer between young and old Syrian golden hamsters. In Vivo. 2005;19(3):639-41.

71. Fu X, Guadagni F, Hoffman RM. A metastatic nude-mouse model of human pancreatic cancer constructed orthotopically with histologically intact patient specimens. Proc Natl Acad Sci U S A. 1992;89(12):5645-9.

72. Farré L, Casanova I, Guerrero S, Trias M, Capellá G, Mangues R. Heterotopic implantation alters the regulation of apoptosis and the cell cycle and generates a new metastatic site in a human pancreatic tumor xenograft model. FASEB J. 2002;16(9):975-82.

73. Morioka CY, Saito S, Ohzawa K, Asano S, Hibino Y, Nakada Y, et al. Subcutaneously inoculated cells and implanted pancreatic cancer tissue show different patterns of metastases in Syrian golden hamsters. JOP. 2000;1(4):183-90.

74. Hotz HG, Hines OJ, Foitzik T, Reber HA. Animal models of exocrine pancreatic cancer. Int J Colorectal Dis. 2000;15(3):136-43.

75. Villarroel MC, Rajeshkumar NV, Garrido-Laguna I, De Jesus-Acosta A, Jones S, Maitra A, et al. Personalizing cancer treatment in the age of global genomic analyses: PALB2 gene mutations and the response to DNA damaging agents in pancreatic cancer. Mol Cancer Ther. 2011;10(1):3-8.

76. Siegel R, DeSantis C, Virgo K, Stein K, Mariotto A, Smith T, et al. Cancer treatment and survivorship statistics, 2012. CA Cancer J Clin. 2012;62(4):220-41.

77. Silverman DT, Brown LM, Hoover RN, Schiffman M, Lillemoe KD, Schoenberg JB, et al. Alcohol and pancreatic cancer in blacks and whites in the United States. Cancer Res. 1995;55(21):4899-905.

78. Ahrendt SA, Pitt HA. Surgical management of pancreatic cancer. Oncology (Williston Park). 2002;16(6):725-34; discussion 34, 36-8, 40, 43.

79. Papac RJ. Origins of cancer therapy. Yale J Biol Med. 2001;74(6):391-8.

80. DeVita VT, Chu E. A history of cancer chemotherapy. Cancer Res. 2008;68(21):8643-53.

81. Gray MJ, Wey JS, Belcheva A, McCarty MF, Trevino JG, Evans DB, et al. Neuropilin-1 suppresses tumorigenic properties in a human pancreatic adenocarcinoma cell line lacking neuropilin-1 coreceptors. Cancer Res. 2005;65(9):3664-70.

82. Khanbolooki S, Nawrocki ST, Arumugam T, Andtbacka R, Pino MS, Kurzrock R, et al. Nuclear factor-kappaB maintains TRAIL resistance in human pancreatic cancer cells. Mol Cancer Ther. 2006;5(9):2251-60.

83. Nawrocki ST, Sweeney-Gotsch B, Takamori R, McConkey DJ. The proteasome inhibitor bortezomib enhances the activity of docetaxel in orthotopic human pancreatic tumor xenografts. Mol Cancer Ther. 2004;3(1):59-70.

84. Geissler C, Hambek M, Eckardt A, Arnoldner C, Diensthuber M, Stöver T, et al. The role of recombinant epidermal growth factor and serotonin in the stimulation of tumor growth in a SCCHN xenograft model. Oncol Rep. 2012;28(3):785-90.

85. Fridman R, Benton G, Aranoutova I, Kleinman HK, Bonfil RD. Increased initiation and growth of tumor cell lines, cancer stem cells and biopsy material in mice using basement membrane matrix protein (Cultrex or Matrigel) co-injection. Nat Protoc. 2012;7(6):1138-44.

86. Fridman R, Giaccone G, Kanemoto T, Martin GR, Gazdar AF, Mulshine JL. Reconstituted basement membrane (matrigel) and laminin can enhance the tumorigenicity and the drug resistance of small cell lung cancer cell lines. Proc Natl Acad Sci U S A. 1990;87(17):6698-702.

87. Bao L, Matsumura Y, Baban D, Sun Y, Tarin D. Effects of inoculation site and Matrigel on growth and metastasis of human breast cancer cells. Br J Cancer. 1994;70(2):228-32.

88. Pepper AR, Gala-Lopez B, Pawlick R, Merani S, Kin T, Shapiro AM. A prevascularized subcutaneous device-less site for islet and cellular transplantation. Nat Biotechnol. 2015;33(5):518-23.

89. Euhus DM, Hudd C, LaRegina MC, Johnson FE. Tumor measurement in the nude mouse. J Surg Oncol. 1986;31(4):229-34.

90. Kuperwasser C, Chavarria T, Wu M, Magrane G, Gray JW, Carey L, et al. Reconstruction of functionally normal and malignant human breast tissues in mice. Proc Natl Acad Sci U S A. 2004;101(14):4966-71.

91. Patel GK, Yee CL, Yuspa SH, Vogel JC. A humanized stromal bed is required for engraftment of isolated human primary squamous cell carcinoma cells in immunocompromised mice. J Invest Dermatol. 2012;132(2):284-90.

92. Williams SA, Anderson WC, Santaguida MT, Dylla SJ. Patient-derived xenografts, the cancer stem cell paradigm, and cancer pathobiology in the 21st century. Lab Invest. 2013;93(9):970-82.

93. Siolas D, Hannon GJ. Patient-derived tumor xenografts: transforming clinical samples into mouse models. Cancer Res. 2013;73(17):5315-9.

94. Tentler JJ, Tan AC, Weekes CD, Jimeno A, Leong S, Pitts TM, et al. Patient-derived tumour xenografts as models for oncology drug development. Nat Rev Clin Oncol. 2012;9(6):338-50.

95. Julien S, Merino-Trigo A, Lacroix L, Pocard M, Goéré D, Mariani P, et al. Characterization of a large panel of patient-derived tumor xenografts representing the clinical heterogeneity of human colorectal cancer. Clin Cancer Res. 2012;18(19):5314-28.

96. Ledford H. Translational research: 4 ways to fix the clinical trial. Nature. 2011;477(7366):526-8.

97. Jin K, Teng L, Shen Y, He K, Xu Z, Li G. Patient-derived human tumour tissue xenografts in immunodeficient mice: a systematic review. Clin Transl Oncol. 2010;12(7):473-80.

98. National Cancer Institute. Available at http://www.cancer.gov/about-cancer/treatment/drugs/fda-erlotinib-hydrochloride2005.

99. Damaraju VL, Scriver T, Mowles D, Kuzma M, Ryan AJ, Cass CE, et al. Erlotinib, gefitinib, and vandetanib inhibit human nucleoside transporters and protect cancer cells from gemcitabine cytotoxicity. Clin Cancer Res. 2014;20(1):176-86.

100. Curt GA, Chabner BA. One in five cancer clinical trials is published: a terrible symptom--what's the diagnosis? Oncologist. 2008;13(9):923-4.

101. Bhowmick NA, Neilson EG, Moses HL. Stromal fibroblasts in cancer initiation and progression. Nature. 2004;432(7015):332-7.

102. Han C, Shen J, Wang H, Yu L, Qian X, Liu B, et al. Personalized primary tumor xenograft model established for the pre-clinical trial to guide postoperative chemotherapy. Med Hypotheses. 2012;79(6):705-8.

103. Bondarenko G, Ugolkov A, Rohan S, Kulesza P, Dubrovskyi O, Gursel D, et al. Patient-Derived Tumor Xenografts Are Susceptible to Formation of Human Lymphocytic Tumors. Neoplasia. 2015;17(9):735-41.

104. Zhao X, Liu Z, Yu L, Zhang Y, Baxter P, Voicu H, et al. Global gene expression profiling confirms the molecular fidelity of primary tumor-based orthotopic xenograft mouse models of medulloblastoma. Neuro Oncol. 2012;14(5):574-83.

105. Von Hoff DD, Ervin T, Arena FP, Chiorean EG, Infante J, Moore M, et al. Increased survival in pancreatic cancer with nab-paclitaxel plus gemcitabine. N Engl J Med. 2013;369(18):1691-703.

106. Apte MV, Park S, Phillips PA, Santucci N, Goldstein D, Kumar RK, et al. Desmoplastic reaction in pancreatic cancer: role of pancreatic stellate cells. Pancreas. 2004;29(3):179-87.

107. Merika EE, Syrigos KN, Saif MW. Desmoplasia in pancreatic cancer. Can we fight it? Gastroenterol Res Pract. 2012;2012:781765.

108. Kimura W. [Anatomy of the head of the pancreas and various limited resection procedures for intraductal papillary-mucinous tumors of the pancreas]. Nihon Geka Gakkai Zasshi. 2003;104(6):460-70.

109. Kimura W. Surgical anatomy of the pancreas for limited resection. J Hepatobiliary Pancreat Surg. 2000;7(5):473-9.

110. Tawada K, Yamaguchi T, Kobayashi A, Ishihara T, Sudo K, Nakamura K, et al. Changes in tumor vascularity depicted by contrast-enhanced ultrasonography as a predictor of chemotherapeutic effect in patients with unresectable pancreatic cancer. Pancreas. 2009;38(1):30-5.

111. Burris HA, Moore MJ, Andersen J, Green MR, Rothenberg ML, Modiano MR, et al. Improvements in survival and clinical benefit with gemcitabine as first-line therapy for patients with advanced pancreas cancer: a randomized trial. J Clin Oncol. 1997;15(6):2403-13.

112. Surveillance, Epidemiology, and End Result Program. National Cancer Institue. Available at http://seer.cancer.gov/statfacts/html/pancreas.html2016.

113. Moore MJ, Goldstein D, Hamm J, Figer A, Hecht JR, Gallinger S, et al. Erlotinib plus gemcitabine compared with gemcitabine alone in patients with advanced pancreatic cancer: a phase III trial of the National Cancer Institute of Canada Clinical Trials Group. J Clin Oncol. 2007;25(15):1960-6.

114. Conroy T, Desseigne F, Ychou M, Bouché O, Guimbaud R, Bécouarn Y, et al. FOLFIRINOX versus gemcitabine for metastatic pancreatic cancer. N Engl J Med. 2011;364(19):1817-25.

115. Kindler HL, Ioka T, Richel DJ, Bennouna J, Létourneau R, Okusaka T, et al. Axitinib plus gemcitabine versus placebo plus gemcitabine in patients with advanced pancreatic adenocarcinoma: a double-blind randomised phase 3 study. Lancet Oncol. 2011;12(3):256-62.

116. Rothenberg ML, Moore MJ, Cripps MC, Andersen JS, Portenoy RK, Burris HA, et al. A phase II trial of gemcitabine in patients with 5-FU-refractory pancreas cancer. Ann Oncol. 1996;7(4):347-53.

117. Spratlin J, Sangha R, Glubrecht D, Dabbagh L, Young JD, Dumontet C, et al. The absence of human equilibrative nucleoside transporter 1 is associated with reduced survival in patients with gemcitabine-treated pancreas adenocarcinoma. Clin Cancer Res. 2004;10(20):6956-61.

118. Plunkett W, Huang P, Gandhi V. Preclinical characteristics of gemcitabine. Anticancer Drugs. 1995;6 Suppl 6:7-13.

119. Spratlin JL, Mackey JR. Human Equilibrative Nucleoside Transporter 1 (hENT1) in Pancreatic Adenocarcinoma: Towards Individualized Treatment Decisions. Cancers (Basel). 2010;2(4):2044-54.

120. Damaraju VL, Kuzma M, Mowles D, Cass CE, Sawyer MB. Interactions of multitargeted kinase inhibitors and nucleoside drugs: Achilles heel of combination therapy? Mol Cancer Ther. 2015;14(1):236-45.

121. Paproski RJ, Young JD, Cass CE. Predicting gemcitabine transport and toxicity in human pancreatic cancer cell lines with the positron emission tomography tracer 3'-deoxy-3'-fluorothymidine. Biochem Pharmacol. 2010;79(4):587-95.

122. Wilson DB. Immunology: Insulin auto-antigenicity in type 1 diabetes. Nature. 2005;438(7067):E5; discussion E-6.

123. Yoon JW, Jun HS. Autoimmune destruction of pancreatic beta cells. Am J Ther. 2005;12(6):580-91.

124. Hypoglycemia in the Diabetes Control and Complications Trial. The Diabetes Control and Complications Trial Research Group. Diabetes. 1997;46(2):271-86.

125. The effect of intensive treatment of diabetes on the development and progression of long-term complications in insulin-dependent diabetes mellitus. The Diabetes Control and Complications Trial Research Group. N Engl J Med. 1993;329(14):977-86.

126. Bruni A, Gala-Lopez B, Pepper AR, Abualhassan NS, Shapiro AJ. Islet cell transplantation for the treatment of type 1 diabetes: recent advances and future challenges. Diabetes Metab Syndr Obes. 2014;7:211-23.

127. Peter A. Senior, Tatsuya Kin, James Shapiro, Koh A. Islet Transplantation at the University of Alberta: Status Update and Review of Progress over the Last Decade. Can J Diabetes 2012. p. 32-7.

128. Shapiro AM. Strategies toward single-donor islets of Langerhans transplantation. Curr Opin Organ Transplant. 2011;16(6):627-31.

129. Pepper AR, Gala-Lopez B, Ziff O, Shapiro AJ. Current status of clinical islet transplantation. World J Transplant. 2013;3(4):48-53.

130. Eich T, Eriksson O, Lundgren T, Transplantation NNfCI. Visualization of early engraftment in clinical islet transplantation by positron-emission tomography. N Engl J Med. 2007;356(26):2754-5.

131. Goto M, Tjernberg J, Dufrane D, Elgue G, Brandhorst D, Ekdahl KN, et al. Dissecting the instant blood-mediated inflammatory reaction in islet xenotransplantation. Xenotransplantation. 2008;15(4):225-34.

132. Nilsson B, Ekdahl KN, Korsgren O. Control of instant blood-mediated inflammatory reaction to improve islets of Langerhans engraftment. Curr Opin Organ Transplant. 2011;16(6):620-6.

133. Pileggi A, Molano RD, Ricordi C, Zahr E, Collins J, Valdes R, et al. Reversal of diabetes by pancreatic islet transplantation into a subcutaneous, neovascularized device. Transplantation. 2006;81(9):1318-24.

134. Lai Y, Schneider D, Kidszun A, Hauck-Schmalenberger I, Breier G, Brandhorst D, et al. Vascular endothelial growth factor increases functional beta-cell mass by improvement of angiogenesis of isolated human and murine pancreatic islets. Transplantation. 2005;79(11):1530-6.

135. Van Deijnen JH, Van Suylichem PT, Wolters GH, Van Schilfgaarde R. Distribution of collagens type I, type III and type V in the pancreas of rat, dog, pig and man. Cell Tissue Res. 1994;277(1):115-21.

136. Wang RN, Paraskevas S, Rosenberg L. Characterization of integrin expression in islets isolated from hamster, canine, porcine, and human pancreas. J Histochem Cytochem. 1999;47(4):499-506.

137. Stendahl JC, Kaufman DB, Stupp SI. Extracellular matrix in pancreatic islets: relevance to scaffold design and transplantation. Cell Transplant. 2009;18(1):1-12.

138. Wang RN, Rosenberg L. Maintenance of beta-cell function and survival following islet isolation requires re-establishment of the islet-matrix relationship. J Endocrinol. 1999;163(2):181-90.

139. Rosenberg L, Wang R, Paraskevas S, Maysinger D. Structural and functional changes resulting from islet isolation lead to islet cell death. Surgery. 1999;126(2):393-8.

140. Pinkse GG, Bouwman WP, Jiawan-Lalai R, Terpstra OT, Bruijn JA, de Heer E. Integrin signaling via RGD peptides and anti-beta1 antibodies confers resistance to apoptosis in islets of Langerhans. Diabetes. 2006;55(2):312-7.

141. Bosco D, Meda P, Halban PA, Rouiller DG. Importance of cell-matrix interactions in rat islet beta-cell secretion in vitro: role of alpha6beta1 integrin. Diabetes. 2000;49(2):233-43.

142. Folkman J, Klagsbrun M, Sasse J, Wadzinski M, Ingber D, Vlodavsky I. A heparin-binding angiogenic protein--basic fibroblast growth factor--is stored within basement membrane. Am J Pathol. 1988;130(2):393-400.

143. Ziolkowski AF, Popp SK, Freeman C, Parish CR, Simeonovic CJ. Heparan sulfate and heparanase play key roles in mouse β cell survival and autoimmune diabetes. J Clin Invest. 2012;122(1):132-41.

144. Olerud J, Mokhtari D, Johansson M, Christoffersson G, Lawler J, Welsh N, et al. Thrombospondin-1: an islet endothelial cell signal of importance for β-cell function. Diabetes. 2011;60(7):1946-54.

145. Johansson A, Lau J, Sandberg M, Borg LA, Magnusson PU, Carlsson PO. Endothelial cell signalling supports pancreatic beta cell function in the rat. Diabetologia. 2009;52(11):2385-94.

146. Daoud J, Petropavlovskaia M, Rosenberg L, Tabrizian M. The effect of extracellular matrix components on the preservation of human islet function in vitro. Biomaterials. 2010;31(7):1676-82.

147. Nagata N, Gu Y, Hori H, Balamurugan AN, Touma M, Kawakami Y, et al. Evaluation of insulin secretion of isolated rat islets cultured in extracellular matrix. Cell Transplant. 2001;10(4-5):447-51.

148. Lucas-Clerc C, Massart C, Campion JP, Launois B, Nicol M. Long-term culture of human pancreatic islets in an extracellular matrix: morphological and metabolic effects. Mol Cell Endocrinol. 1993;94(1):9-20.

149. Jalili RB, Moeen Rezakhanlou A, Hosseini-Tabatabaei A, Ao Z, Warnock GL, Ghahary A. Fibroblast populated collagen matrix promotes islet survival and reduces the number of islets required for diabetes reversal. J Cell Physiol. 2011;226(7):1813-9.

150. Zhang Y, Jalili RB, Warnock GL, Ao Z, Marzban L, Ghahary A. Three-dimensional scaffolds reduce islet amyloid formation and enhance survival and function of cultured human islets. Am J Pathol. 2012;181(4):1296-305.

151. Pedraza E, Brady AC, Fraker CA, Molano RD, Sukert S, Berman DM, et al. Macroporous three-dimensional PDMS scaffolds for extrahepatic islet transplantation. Cell Transplant. 2013;22(7):1123-35.

152. Salvay DM, Rives CB, Zhang X, Chen F, Kaufman DB, Lowe WL, et al. Extracellular matrix protein-coated scaffolds promote the reversal of diabetes after extrahepatic islet transplantation. Transplantation. 2008;85(10):1456-64.

153. Sionov RV, Finesilver G, Sapozhnikov L, Soroker A, Zlotkin-Rivkin E, Saad Y, et al. Beta Cells Secrete Significant and Regulated Levels of Insulin for Long Periods when Seeded onto Acellular Micro-Scaffolds. Tissue Eng Part A. 2015;21(21-22):2691-702.

154. Shamis Y, Hasson E, Soroker A, Bassat E, Shimoni Y, Ziv T, et al. Organ-specific scaffolds for in vitro expansion, differentiation, and organization of primary lung cells. Tissue Eng Part C Methods. 2011;17(8):861-70.

155. Motta PM, Macchiarelli G, Nottola SA, Correr S. Histology of the exocrine pancreas. Microsc Res Tech. 1997;37(5-6):384-98.

156. Song JJ, Ott HC. Organ engineering based on decellularized matrix scaffolds. Trends Mol Med. 2011;17(8):424-32.

157. Kin T, Senior P, O'Gorman D, Richer B, Salam A, Shapiro AM. Risk factors for islet loss during culture prior to transplantation. Transplant international : official journal of the European Society for Organ Transplantation. 2008;21(11):1029-35.

158. Ricordi C, Lacy PE, Scharp DW. Automated islet isolation from human pancreas. Diabetes. 1989;38 Suppl 1:140-2.

159. Nagata NA, Inoue K, Tabata Y. Co-culture of extracellular matrix suppresses the cell death of rat pancreatic islets. J Biomater Sci Polym Ed. 2002;13(5):579-90.

160. Bretland AJ, Lawry J, Sharrard RM. A study of death by anoikis in cultured epithelial cells. Cell Prolif. 2001;34(4):199-210.

161. Frisch SM, Screaton RA. Anoikis mechanisms. Curr Opin Cell Biol. 2001;13(5):555-62.

162. Thomas FT, Contreras JL, Bilbao G, Ricordi C, Curiel D, Thomas JM. Anoikis, extracellular matrix, and apoptosis factors in isolated cell transplantation. Surgery. 1999;126(2):299-304.

163. Hammar E, Parnaud G, Bosco D, Perriraz N, Maedler K, Donath M, et al. Extracellular matrix protects pancreatic beta-cells against apoptosis: role of short- and long-term signaling pathways. Diabetes. 2004;53(8):2034-41.

164. Rücker M, Laschke MW, Junker D, Carvalho C, Schramm A, Mülhaupt R, et al. Angiogenic and inflammatory response to biodegradable scaffolds in dorsal skinfold chambers of mice. Biomaterials. 2006;27(29):5027-38.

165. Kawahara T, Kin T, Kashkoush S, Gala-Lopez B, Bigam DL, Kneteman NM, et al. Portal vein thrombosis is a potentially preventable complication in clinical islet transplantation. Am J Transplant. 2011;11(12):2700-7.

166. Ao Z, Matayoshi K, Lakey JR, Rajotte RV, Warnock GL. Survival and function of purified islets in the omental pouch site of outbred dogs. Transplantation. 1993;56(3):524-9.

167. Wahoff DC, Sutherland DE, Hower CD, Lloveras JK, Gores PF. Free intraperitoneal islet autografts in pancreatectomized dogs--impact of islet purity and posttransplantation exogenous insulin. Surgery. 1994;116(4):742-8; discussion 8-50.

168. Fritschy WM, van Straaten JF, de Vos P, Strubbe JH, Wolters GH, van Schilfgaarde R. The efficacy of intraperitoneal pancreatic islet isografts in the reversal of diabetes in rats. Transplantation. 1991;52(5):777-83.

169. Lorenz D, Reding R, Petermann J, Lippert H, Worm V, Tietz W, et al. Transplantation of isologous islets of Langerhans in diabetic rats. Long-term immunohistochemical results. Acta Diabetol Lat. 1977;14(5-6):199-210.

170. Ryan EA, Paty BW, Senior PA, Bigam D, Alfadhli E, Kneteman NM, et al. Five-year follow-up after clinical islet transplantation. Diabetes. 2005;54(7):2060-9.